Elastic Growth Models

Alain Goriely, Mark Robertson-Tessi, Michael Tabor, Rebecca Vandiver

Program in Applied Mathematics, RUMMBA (Research Unit in Mathematics, Mechanics, Biology, and Applications), University of Arizona, Tucson AZ85721
goriely@math.arizona.edu

Summary. Growth is involved in many fundamental biological processes such as morphogenesis, physiological regulation, or pathological disorders. It is, in general, a process of enormous complexity involving genetic, biochemical, and physical components at many different scales and with complex interactions. The purpose of this paper is to provide a simple introduction to the modeling of elastic growth. We first consider systems in one-dimensions (suitable to model filamentary structures)to introduce the key concepts. Second, we review the general three-dimensional theory and show how to apply it to the growth of cylindrical structures. Different possible growth mechanisms are considered.

Key words: Biological growth, growing rods, morphoelasticity, Mooney-Rivlin material.

1 Introduction

Biological growth is a fascinating process of tremendous complexity that has attracted the attention of generations of biologists and remains today a fundamental scientific problem. Surprisingly, this problem has met with little interest in the physics and mathematics community. However, with the development of quantitative biomechanics (in the footsteps of scientists like Skalak and Fung), the mathematical development of exact elasticity, the physical modeling of growth, and computational advances, a theory of growth has emerged and the mathematical analysis of its consequences is finally possible. The purpose of this article is to provide an introduction to the problem of growth, its mathematical issues and the scientific challenges ahead of us.

The emphasis will be on the particular role played by mechanical quantities (such as stresses and strains) and their interaction with changes in geometry arising during growth. Based on these observations and simple mechanical systems in one dimension we will discuss different approaches to modeling macroscopic growth in continuum mechanics and show how to generalize the

classical theory of exact elasticity. The mathematical analysis of such a theory of growth enables us to understand the particular interaction between geometry and mechanics and helps us to identify particular mechanisms that can be used either in building specific material properties, in homeostatic regulation, or in embryonic development through instability-driven pattern formation.

2 One-dimensional Theory: Elasticity, Visco-elasticity, and Plasticity

We start with a simple conceptual framework by considering growth phenomena in one dimension. That is, we consider the growth of a (mostly) filamentary structure. This type of growth is found in many microbial systems such as filamentous bacteria and fungi but also in plants where stems, roots, and tendrils all display some aspects of one-dimensional growth. In size, these systems span at least 6 orders of magnitude from microns to meters. Biologists would be quick (and correct) to point out that growth in these systems is much more complex and involves structural details at the wall level which are necessary to describe any features related to growth. Here we choose to look at these systems as a mechanical continuum for which some features and time-evolution are dominated by its slenderness and hence can be modeled as elastic filaments.

Before reviewing the published plant growth models it is useful to recall the basic facts about Kelvin solids, Maxwell fluids, and Bingham fluids.

2.1 Kelvin Solids

A purely elastic material is one in which the response to applied stresses is instantaneous and reversible. A Kelvin solid is an elastic solid but one in which the response to the stress occurs over a finite time determined by the viscous characteristic of the "solid". In the simplest one dimensional case, one can write

$$\sigma = E\epsilon + \eta\frac{\pi\epsilon}{\pi t}, \tag{1}$$

where σ denotes the (applied) stress, and ϵ denotes strain. E is an elastic modulus and η a coefficient of viscosity. If $\eta = 0$ the equation reduces to the classical constitutive relation for an elastic solid. If $\eta \neq 0$, the basic idea can be illustrated by the case of a constant applied stress σ_0.

$$\sigma_0 = E\epsilon + \eta\frac{\pi\epsilon}{\pi t}. \tag{2}$$

The equation is easily solved for ϵ to give

$$\epsilon(t) = \frac{\sigma_0}{E}\left(1 - e^{-t/\tau_r}\right), \tag{3}$$

where

$$\tau_r = \eta/E, \tag{4}$$

is the "visco-elastic" relaxation time. Another standard exercise is to impose a periodic stress $\sigma(t) = \sigma_0 \cos(\omega t)$ which gives, in the limit $t \to \infty$

$$\epsilon(t) = \frac{\sigma_0 E}{E^2 + \eta^2 E^2} \cos(\omega t - \alpha), \tag{5}$$

which shows a phase lag α between the strain and the applied stress, where

$$\alpha = \arctan(\tau_r/\tau_\sigma), \tag{6}$$

represents the competition between the response time of the solid $\tau_r = \eta/E$ and the time scale of the applied stress $\tau_\sigma = 1/\omega$. One should also note that if the stress is suddenly turned off, the strain relaxes as

$$\epsilon \sim e^{-t/\tau_r}. \tag{7}$$

2.2 Maxwell Fluids

A Maxwell fluid is a viscous fluid with some elastic properties. The simplest model is one in which the *rate of strain* obeys the equation

$$\frac{\pi\epsilon}{\pi t} = \frac{1}{\eta}\sigma + \frac{1}{E}\frac{\pi\sigma}{\pi t}. \tag{8}$$

Three simple comments:

1. If the second term on the r.h.s is dropped one is left with the simplest fluid model
$$\frac{\pi\epsilon}{\pi t} = \frac{1}{\eta}\sigma, \tag{9}$$
in which rate of strain is proportional to the stress and the fluid exhibits irreversible flow.
2. If the first term on the r.h.s. is dropped one is left with
$$\frac{\pi\epsilon}{\pi t} = \frac{1}{E}\frac{\pi\sigma}{\pi t}, \tag{10}$$
which represents the elastic component of the material: after integrating both sides w.r.t. time one simply has the pure elastic response $\epsilon = \sigma/E$.
3. If the strain is turned off, the stress relaxes as
$$\sigma \sim e^{-t/\tau_r}, \tag{11}$$
where τ_r is as above - which should be contrasted with the equivalent strain relaxation of a Kelvin solid when the stress is turned off.

Basic features of the Maxwell model can be illustrated with an applied stress of the form

$$\sigma = \sigma_0 \left(1 - e^{-t/T}\right). \tag{12}$$

If T is small the stress ramps up rapidly; if T is large, the stress ramps up slowly. The rate of strain equation can be integrated explicitly to give

$$\epsilon(t) = \frac{\sigma_0}{\eta}\left(t + T\left(e^{-t/T} - 1\right)\right) + \frac{\sigma_0}{E}\left(1 - e^{-t/T}\right). \tag{13}$$

(i) For the case $0 < t < T$, with T small, *i.e.* for short times in the case of a rapidly ramped stress, one finds that

$$\epsilon \sim \frac{\sigma_0}{ET} t, \tag{14}$$

which shows that the strain follows the applied stress according the elastic part of the system, $\dot{\epsilon} \sim \dot{\sigma}/E$.
(ii) For $t \gg T$, one finds that

$$\epsilon \sim \frac{\sigma_0}{\eta} t, \tag{15}$$

which shows that the strain is dominated by the fluid component of the system, $\dot{\epsilon} \sim \sigma/\eta$.

2.3 Bingham Fluids

In a simple fluid there is (irreversible) flow in response to applied stress, however small. For non-Newtonian fluids such as paint, flow does not begin until a critical yield stress, σ^*, has been exceeded. This is the Bingham model which, in its simplest form, is expressed as

$$\frac{\pi\epsilon}{\pi t} = \frac{1}{\nu}[\sigma - \sigma^*], \tag{16}$$

where $[\sigma - \sigma^*] = \max(0, (\sigma - \sigma^*))$. This model of irreversible extension (flow) once a critical stress has been exceeded, has been the paradigm for most plant growth models. The Bingham model can easily be generalized to a Maxwell-Bingham type system represented by

$$\frac{\pi\epsilon}{\pi t} = \frac{1}{\nu}[\sigma - \sigma^*] + \frac{1}{E}\frac{\pi\sigma}{\pi t}. \tag{17}$$

In terms of terminology, the convention is (or should be!) to call a Maxwell fluid *visco-elastic*, reflecting the combination of irreversible flow generated by viscous stresses with an elastic component; and to term a Bingham fluid *plastic* - a much misused term which is (or should) be used to mean an irreversible deformation beyond a critical yield stress. A comparison of the strains produced by the different models is given in Fig.1).

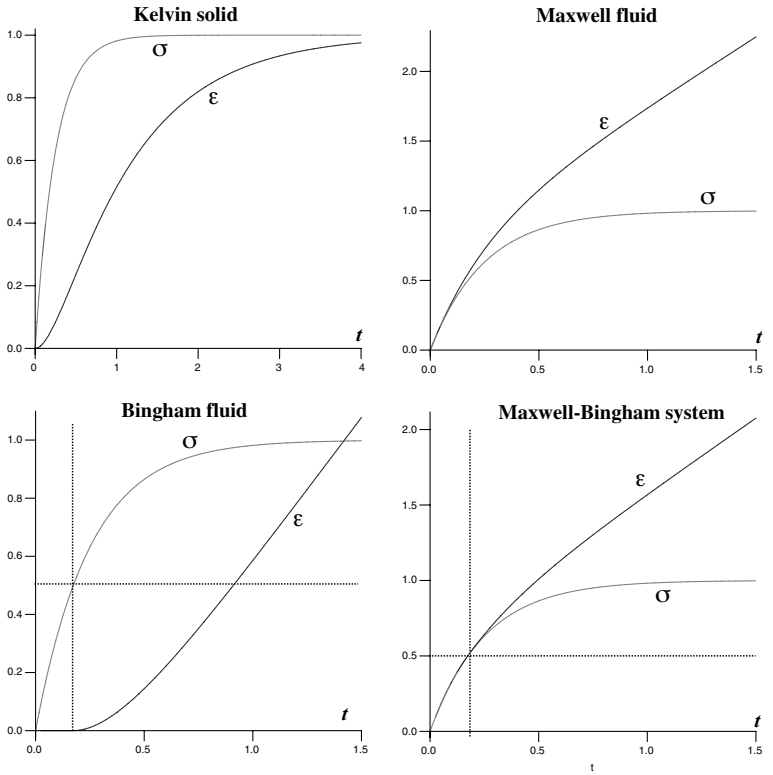

Fig. 1. Comparison of strains produced by a ramping of the stress for four different materials, $\nu = 1/4, \sigma^* = 1/2, E = \sigma_0 = \eta = 1, T = 1/4$.

3 One-dimensional Theory: Growth Models

3.1 Lockhart-Ortega-Cosgrove Model

Lockhart's model is one of the earliest quantitative models of plant cell growth [45]. Geometrically the plant cell is considered to be an axisymmetric cylinder of constant radius, but growing length. This growth in length is related to the increase in volume due to water entering the cell, and the irreversible length increase is, in turn, taken to be the result of the turgor pressure exerted on the cell wall (in fact, in this model, this is the pressure exerted on the end of cylinder which is treated as a flat cap). Lockhart's discussion begins with a seemingly simple statement about the elastic strain in the system which he defines as

$$\epsilon = \frac{l - l_0}{l_0}, \tag{18}$$

and is governed by a simple Hooke's law, namely

$$\epsilon = \frac{1}{E}\sigma. \tag{19}$$

Assuming a constant applied stress σ, time differentiation of the strain gives

$$\dot{\epsilon} = \frac{\dot{l}}{l_0} - \frac{l}{l_0}\frac{\dot{l_0}}{l_0} = 0, \tag{20}$$

and hence

$$\frac{\dot{l}}{l} = \frac{\dot{l_0}}{l_0}. \tag{21}$$

In terms of our own language, what does this mean? If we regard l as the current length and l_0 as the reference length, then if both are growing in time, a constant rate of strain can be maintained if the reference length extends elastically, at each instant, the same amount as the current length. Lockhart points out that the time scale of elastic equilibrium for plant cells (minutes) is much more rapid than the time scale of the irreversible extension (hours); hence the system is claimed to always be in a state of elastic equilibrium as it grows. Lockhart's argument proceeds in two parts. The increase in (current) length due to volume increase (due to osmosis) is expressed as

$$\frac{dl}{dt} = \frac{KA}{a}(\Delta\Pi - P) \tag{22}$$

where K is a water permeability constant, $A = 2\pi rl$ is the cylinder side wall area, $a = \pi r^2$ the cross-sectional area, $\Delta\Pi$ an osmotic pressure variable, and P the turgor pressure. This is re-expressed as

$$\frac{1}{l}\frac{dl}{dt} = \frac{2K}{r}(\Delta\Pi - P). \tag{23}$$

The left hand side $\dot{l}/l$ could be thought of as a "current configuration rate of strain". He then goes on to define the "irreversible wall extension" as

$$\frac{1}{l_0}\frac{dl_0}{dt} = \Phi\sigma, \tag{24}$$

where Φ characterizes the cell wall's "rate of irreversible flow" (Lockhart's terminology). A few comments: (i) the left hand side $\dot{l_0}/l_0$ could be thought of as a "reference configuration rate of strain" - from the point of view of a growth process it may indeed be appropriate to measure the growth in terms of the change in reference configuration length; (ii) the equation of motion represents a simple fluid flow (*i.e.* rate of strain $\propto$ stress); (iii) as Lockhart points out (24) could be modified to correspond to a Bingham type flow, namely

$$\frac{1}{l_0}\frac{dl_0}{dt} = \Phi[\sigma - \sigma^*]. \tag{25}$$

The stress σ is expressed, in the standard way, in terms of the (turgor) pressure on the end cap and the wall thickness, δ, *i.e.* $\sigma = \pi r^2 P / 2\pi r\delta$. The equation of motion (24) is then used to express P in terms of the extension, namely

$$P = \frac{2\delta}{r\Phi}\frac{1}{l_0}\frac{dl_0}{dt} = \frac{2\delta}{r\Phi}\frac{1}{l}\frac{dl}{dt}, \tag{26}$$

where (21) is used to obtain the last equality. This expression for P is then combined with (23) to give

$$\frac{1}{l}\frac{dl}{dt} = \frac{2rK\Delta\Pi\Phi}{4\delta K + r^2\Phi}, \tag{27}$$

which is essentially Lockhart's main result (introducing a Bingham type flow only modifies the equation slightly) which, in the end, relates the current rate of strain to a stress representing the interplay of osmotic and turgor pressures. The various way in which strain, and rates of strain, are defined - and then connected through the assumption of constant elastic strain - is not especially satisfactory. We also note (see below) that the equation does not depend on the elastic modulus of the system.

The assumed state of constant elastic equilibrium is a consequence of the assumed constancy of the stresses. This means that the constitutive relation (24) is simply that of a (simple) fluid. Ortega proposed that the effect of elasticity can be explicitly restored by replacing (24)or (25) by a Maxwell type relationship [58], namely

$$\frac{de}{dt} = \Phi[\sigma - \sigma^*] + \frac{1}{E}\frac{d\sigma}{dt}, \tag{28}$$

where de/dt is the elongation strain rate which Ortega defines as $de/dt = (1/l)dl/dt$. Ortega's analysis of his model yields some interesting extensions of Lockhart's model - which we shall not pursue here. A somewhat similar discussion/extension of Lockhart's model was also given by Cosgrove [11].

3.2 Goodwin Model

Goodwin [22] begins by summarizing the Lockhart-Cosgrove-Ortega model in the form

$$\frac{1}{V}\frac{dV}{dt} = \phi[P - Y] + \frac{1}{E}\frac{dP}{dt}, \tag{29}$$

where he describes Y as the yield threshold, ϕ as the extensibility coefficient of the wall, and E as the volumetric elastic modulus $E = VdP/dV$. Noting that the volumetric growth rate $(1/V)dV/dt$ is analogous to a rate of strain and P corresponds to a mechanical stress, he recasts the equation in the form

$$E\frac{d\epsilon}{dt} = \frac{1}{\tau}[\sigma - Y] + \frac{d\sigma}{dt}, \tag{30}$$

where ϵ is the strain and in the form of a Maxwell-Bingham constitutive relationship. He notes that when $\sigma > Y$, the strain ϵ is a combination of an elastic strain (proportional to the stress variations) and a growth strain Γ, where the rate of growth is expressed as

$$E\frac{d\Gamma}{dt} = \frac{1}{\tau}[\sigma - Y] \tag{31}$$

We see that (30) can be written as

$$\frac{d\epsilon}{dt} = \frac{d\Gamma}{dt} + \frac{1}{E}\frac{d\sigma}{dt}. \tag{32}$$

and as we will see this is the bridge to the three-dimensional growth model by Rodriguez *et al.* described in section 4.1. Goodwin defines the growth rate in terms of the reference length, namely

$$\frac{d\Gamma}{dt} = \frac{1}{l_0}\frac{dl_0}{dt}, \tag{33}$$

and hence the growth rate equation

$$\frac{1}{l_0}\frac{dl_0}{dt} = \frac{1}{\tau}[\epsilon - s], \tag{34}$$

where $s = Y/E$ and the stress σ is expressed in terms of the elastic strain, *i.e.* $\sigma = \epsilon E$, This latter assumption may not be a good physical model. The growth rate equation (34) is now a strain based model, *i.e.* irreversible extension if the elastic strain exceeds a critical *strain* threshold. Goodwin then argues that there could also be a contribution to the growth as a result of a change in the elastic modulus. Thus assuming the Hooke's law $\sigma = E\epsilon$ and differentiating both sides w.r.t. time under the assumption of constant stress gives

$$\frac{d\epsilon}{dt} = -\frac{\epsilon}{E}\frac{dE}{dt}, \tag{35}$$

If the elastic strain ϵ is taken to be $\epsilon = (l - l_0)/l_0$ and that the variations in ϵ is due to changes in l_0 (a proposition that might require a little more thought) then the above relationship can be cast in the form

$$\frac{1}{l_0}\frac{dl_0}{dt} = \frac{\epsilon}{1+\epsilon}\frac{1}{E}\frac{dE}{dt}. \tag{36}$$

If this is added to (34) one has the Goodwin growth rate model

$$\frac{1}{l_0}\frac{dl_0}{dt} = \frac{1}{\tau}[\epsilon - s] + \frac{\epsilon}{1+\epsilon}\frac{1}{E}\frac{dE}{dt}. \tag{37}$$

Two comments: (i) the recognition of a total rate of strain being decomposed in to a growth rate part *analogous to* a simple Bingham fluid flow, and an elastic (rate of strain) part is fundamental to the model and is, in fact, equivalent to the simplest form of Prandtl-Reuss equations for elasto-plastic deformation ; (ii) the separate consideration of the elastic stress variation (35) and then its addition to the growth rate component, could be interpreted as a statement of the widely different time scales of the growth and elastic processes.

3.3 Stein Model

The discussion of (biological) rod growth by A.A. Stein [71] is the most self-consistent of the models to date and, as is quickly apparent, a linearized version of the more general approach of Rodriguez *et. al.* (see section 4.1). His starting point is

$$\dot{\epsilon} = \dot{\epsilon_g} + \dot{\epsilon_e}, \tag{38}$$

which could be interpreted as the total rate of strain, $\dot{\epsilon}$ equals the growth rate $\dot{\epsilon_g}$ plus the elastic rate of strain $\dot{\epsilon_e}$. [1] He proposes that the growth rate takes the general form

$$\dot{\epsilon_g} = A + M\sigma, \tag{39}$$

and the elastic *strain*, ϵ_e, satisfies a Hookean relationship

$$\epsilon_e = K\sigma. \tag{40}$$

In the above three equations all variables are now taken to be tensorial. Given the above, the rest is straight forward. In component form (38) is thus

$$\dot{\epsilon}_{kl} = A_{kl} + M_{klmn}\sigma^{mn} + \frac{d}{dt}\left(M_{klmn}\sigma^{mn}\right). \tag{41}$$

He makes an intriguing aside that since the elastic deformations are so small, the type of time derivative is unimportant, so d/dt can be taken as differentiation w.r.t. time for fixed comoving coordinates, and that use of the Oldroyd derivative instead of this would only add negligibly small corrections. The stresses are assumed to satisfy the standard equilibrium equations

$$\frac{\pi\sigma^{kl}}{\pi x^l} + F^k = 0. \tag{42}$$

Stein first considers the case of a growing rectangular cylinder under pressure yielding simple equations for the growth of the cylinder length (no great surprises found here). It would appear that be defines his (total) rate of strain as $\dot{l}/l$ where l is the current length. He then goes on to tackle the more difficult case of a growing bending rod.

3.4 Growing Cosserat Rods

A rod [2, 10, 47] is represented by its centerline $\mathbf{r}(s)$ where s is a material parameter taken to be the arc length in a stress free configuration ($0 \leq s \leq L$) and two orthonormal vector fields $\mathbf{d}_1(s)$, $\mathbf{d}_2(s)$ representing the orientation of a material cross section at s.

[1] Care must be taken when defining "elastic rate of strain" - a point we will discuss later. (We comment that Stein refers to the various $\dot{\epsilon}$ as "velocity tensors of the [associated]...strains". As a pedantic point - which we will pursue later - we note that velocity gradients and rates of strain are only equivalent in infinitesimal elasticity theory.)

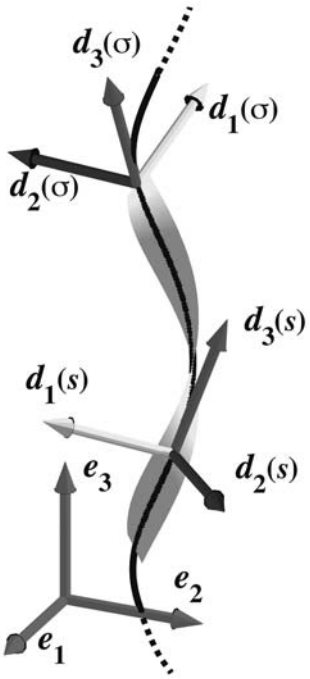

Fig. 2. The director basis represents the evolution of a local basis along the rod.

A local orthonormal basis is obtained (see Fig. 2) by defining $\mathbf{d}_3(s) = \mathbf{d}_1(s) \times \mathbf{d}_2(s)$ and a complete kinetic description is given by:

$$\mathbf{r}' = \mathbf{v}, \tag{43}$$

$$\mathbf{d}_i' = \mathbf{u} \times \mathbf{d}_i, \qquad i = 1, 2, 3, \tag{44}$$

$$\dot{\mathbf{d}}_i = \mathbf{w} \times \mathbf{d}_i \qquad i = 1, 2, 3, \tag{45}$$

where $(\,)'$ and $\dot{(\,)}$ denote the derivative with respect to s and t, and $\mathbf{u}$, $\mathbf{v}$ are the *strain* vectors and $\mathbf{w}$ is the *spin* vector. The components of a vector $\mathbf{a} = \mathsf{a}_1\mathbf{d_1} + \mathsf{a}_2\mathbf{d_2} + \mathsf{a}_3\mathbf{d_3}$ in the local basis are denoted by $\mathbf{a} = (\mathsf{a}_1, \mathsf{a}_2, \mathsf{a}_3)$ (following [2], we use the sans-serif fonts to denote the components of a vector in the local basis). The two first components represent transverse shearing while $\mathsf{v}_3 > 0$ is associated with stretching and compression. The two first components of the *curvature vector* $\mathbf{u}$, are associated with bending while u_3 represents twisting.

The stress acting at $\mathbf{r}(s)$ is given by a resultant force $\mathbf{N}(\mathbf{s})$ and resultant moment $\mathbf{m}(s)$. The balance of linear and angular momenta yields [2]

$$\mathbf{n}' + \mathbf{f} = \rho\mathcal{A}\ddot{\mathbf{r}}, \tag{46}$$

$$\mathbf{m}' + \mathbf{r}' \times \mathbf{n} + \mathbf{l} = \rho\left(I_2\mathbf{d_1} \times \ddot{\mathbf{d}}_\mathbf{1} + I_1\mathbf{d_2} \times \ddot{\mathbf{d}}_\mathbf{2}\right), \tag{47}$$

where $\mathbf{f}(s)$ and $\mathbf{l}(s)$ are the body force and couple per unit length applied on the cross section at s (these body forces and couple can be used to model different effects such as short and long range interactions between different part of the rod or can be the result of self-contact or contact with another body), $\mathcal{A}$ is the cross-section area, ρ the mass density, and $I_{1,2}$ are the principal moments of inertia of the cross section (corresponding to the directions $\mathbf{d}_{1,2}$).

To close the system, we assume that the resultant stresses are related to the strains. There are two important cases to distinguish.

Extensible and Shearable Rods

First, we consider the case where the rod is extensible and shearable and we assume that there exists a strain-energy density function $W = W(\mathbf{y}, \mathbf{z}, s)$ such that the constitutive relations for the resultant moment and force in the local basis are given by

$$\mathbf{m} = f(\mathbf{u} - \hat{\mathbf{u}}, \mathbf{v} - \hat{\mathbf{v}}, s) = \partial_{\mathbf{y}} W(\mathbf{u} - \hat{\mathbf{u}}, \mathbf{v} - \hat{\mathbf{v}}, s), \tag{48}$$

$$\mathbf{n} = g(\mathbf{u} - \hat{\mathbf{u}}, \mathbf{v} - \hat{\mathbf{v}}, s) = \partial_{\mathbf{z}} W(\mathbf{u} - \hat{\mathbf{u}}, \mathbf{v} - \hat{\mathbf{v}}, s), \tag{49}$$

where $\hat{\mathbf{v}}$, $\hat{\mathbf{u}}$ are the strains in the unstressed reference configuration ($\mathbf{m} = \mathbf{n} = 0$ when $\mathbf{u} = \hat{\mathbf{u}}$, $\mathbf{v} = \hat{\mathbf{v}}$). Typically, W is assumed to be continuously differentiable, convex, and coercive. The rod is *uniform* if its material properties do not change along its length (*i.e.* W has no explicit dependence on s) and the stress-free strains $\hat{\mathbf{v}}$, $\hat{\mathbf{u}}$ are independent of s.

Inextensible and Unshearable Rods

In the second case, we assume that the rod is inextensible and unshearable, that is we take $\mathbf{v} = \mathbf{d}_3$ and the material parameter s becomes the arc length. In that case, there is no constitutive relationship for the resultant force and the strain-energy density function is a function only of $(\mathbf{u} - \hat{\mathbf{u}})$, that is

$$\mathbf{m} = \partial_{\mathbf{y}} W(\mathbf{u} - \hat{\mathbf{u}}) = f(\mathbf{u} - \hat{\mathbf{u}}) \tag{50}$$

In the simplest (and most widely used) case the energy is

$$W_1 = K_1 u_1^2 + K_2(u_2 - \hat{u}_2)^2 + K_3(u_3 - \hat{u}_3)^2, \tag{51}$$

where $\hat{u}_2$ and $\hat{u}_3$ represent the intrinsic curvature and torsion that represent the shape of the filament when unloaded. Explicitly, the resultant moment is

$$\mathbf{m} = EI_1 \mathsf{u}_1 \mathbf{d}_1 + EI_2(u_2 - \hat{u}_2)\mathbf{d}_2 + \mu J(u_3 - \hat{u}_3)\mathbf{d}_3 \tag{52}$$

where E is the young modulus, μ is the shear modulus, and J is a parameter that depends on the cross-section shape (an explicit form for J and examples can be found in [29]). For a circular cross-section, these parameters are:

$$I_1 = I_2 = \frac{J}{2} = \frac{\pi R^4}{4}, \tag{53}$$

where R is the radius of the cross-section. The products EI_1 and EI_2 are usually called the *principal bending stiffnesses* of the rod, and μJ is the *torsional stiffness*.

The orthonormal frame $(\mathbf{d_1}, \mathbf{d_2}, \mathbf{d_3})$ is different from the Frenet-Serret frame defined by the triple (normal,binormal,tangent)=$(\boldsymbol{\nu}, \boldsymbol{\beta}, \boldsymbol{\tau})$. If we take $\mathsf{v}_1 = \mathsf{v}_2 = 0,\ \mathsf{v}_3 = 1$, then the vectors $(\mathbf{d_1}, \mathbf{d_2})$ lie in the normal plane to the axis and are related to the normal and binormal vectors by a rotation through an angle φ:

$$\mathbf{d}_1 = \boldsymbol{\nu} \cos\varphi + \boldsymbol{\beta} \sin\varphi \tag{54}$$

$$\mathbf{d}_2 = -\boldsymbol{\nu} \sin\varphi + \boldsymbol{\beta} \cos\varphi \tag{55}$$

This rotation implies that

$$\mathbf{u} = (\kappa \sin\varphi, \kappa \cos\varphi, \tau + \varphi') \tag{56}$$

where κ and τ are the usual Frenet curvature and torsion.

Growing Rods

We are now in a position to model growth in elastic rods. There are actually three different ways that this can be achieved. The first approach, which we refer to as *parameter variation* consists in considering families of rod solutions (typically static due to the slow time evolution of growth with respect to viscous damping in the rod) parametrized by one of the material parameters. For instance, in the growth of a tree, one may consider the length and width as two parameters that evolve in time. At each time, we increase the value of such parameters and recompute the static solution that match the boundary conditions. The second approach is *remodeling*. The idea is now to consider a separate evolution law for the material parameters that may depend on time and history of the material. This is fundamentally different from the previous approach since the material parameters may now be a local function of the position and their values depend on the evolution in time. The third approach is the *evolution of the natural configuration*. This is somewhat more subtle and will open the discussion to the general discussion of growth in three-dimensional nonlinear elasticity.

Growing Rods: Parameter Variation

In this quasi-static approach, each solution remains a solution of the classic Kirchhoff equations and growth is studied by considering the evolution of such solutions w.r.t. the parameters. The idea is to study the evolution of shape

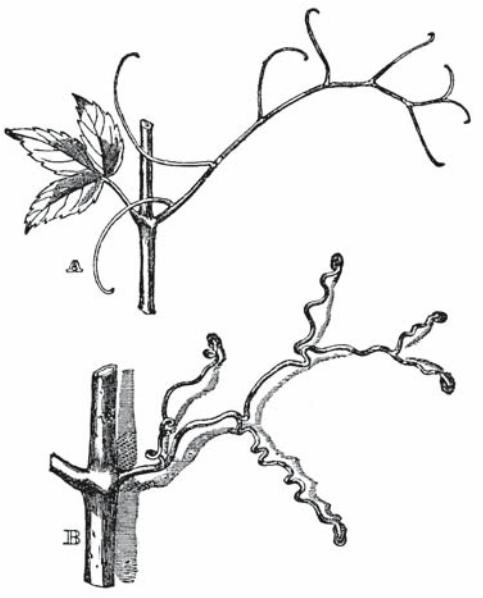

Fig. 3. Growth of a tendril. Once attached the tendril develops a perversion composed of two helical structure with opposite handedness Drawing from [12]. In the first stage (A), the tendrils are *circumnutating* until they find an attachment. In the second stage (B), the tendrils are attached and perversion sets in.

and change in shape through a bifurcation process mediated by a control parameter.

As a first example, consider the evolution of tendrils in plants [28, 50]. A tendril is a modified leaf that can be found at the extremities of some climbing plants and are used by the plants to achieve vertical growth by attaching itself to other supports. A tendril can be modeled as an elastic rod under tension. Once a tendril has grasped a support, it starts developing curvature by differential growth until it bifurcates to a shape made out of 2 (or more) helical structures with opposite handedness called a *perversion* (this is due to the fact that the original structure has no twist and neither ends are allowed to rotate–See Fig.3). These helical springs provide the climbing plant with a firm but elastic connection to its support [12]. The creation of these helical structures from a straight filament can be understood in terms of parameter variation. The tendril is modeled as an initially straight filament under tension. Its constant intrinsic curvature increases slowly in time and the filament is considered to be in static equilibrium at all time. The problem reduces to exploring the possibility of a bifurcation from a straight solution to a solution connecting asymptotically two helical structure of opposite handedness (See Fig. 4).

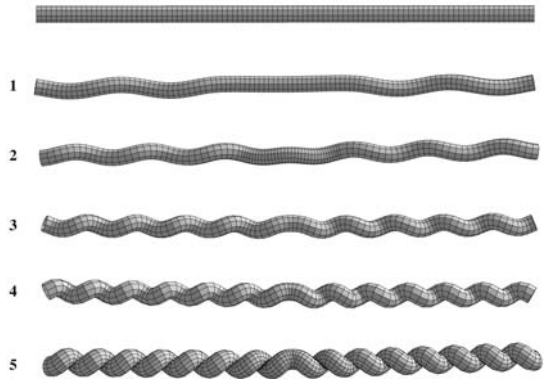

Fig. 4. Model of perversion. A straight rod under tension undergoes a bifurcation when its intrinsic curvature is increased (from top to bottom). Reproduced from [50].

As a second example, consider the growth of twining vines. Twining plants achieve vertical growth by revolving around supports of different sizes on which they exert a pressure. During growth, the growing tip waves around in a circular motion known as circumnutation until it finds an appropriate upright support and then start wrapping around it to extend upward. The tip of the vine keeps nutating and the vine pursue its climbing process by forming a spiral around the support. The growth process of twining plants raises many interesting mechanical questions already noted by 19th century botanists and further studied by Silk, Holbrook and co-workers [48,64,68–70]. Viewed as a growth problem, we can study the possible equilibria of a rod with intrinsic curvature and torsion in contact with a cylinder and with increasing length. Therefore the problem reduces to finding suitable solution with increasing length, taken as our control parameter. There exist many different regimes that can be studied from a bifurcation standpoint, in particular, one can determine the maximal pole radius around which a vine can grow, an interesting question raised by Charles Darwin (1888) (see [25] for details). Here we restrict our attention to the problem of finding a solution that corresponds to the correct mechanical behavior of the plant during growth. That is, the vine connect a helical solution to a hook like structure (termed the *anchor*). Such solutions were found and an example is given in Fig.5.

Another example of growth through parameter variation can be found in [76] where the growth of twisted circular ring with application to the growth of *B. subtilis* was considered (See below).

Growing Rods: Remodeling

In the previous examples, growth was passive. That is, it is modeled by the evolution of an outside control parameter without any feedback from the form to the material parameters. In many growth process, the evolution of the struc-

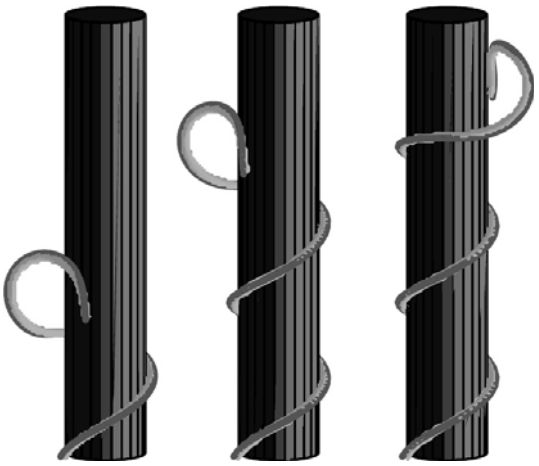

Fig. 5. A sequence of three-dimensional solutions to the attachment problem. Note the continuous, almost helical, solution, followed by the anchor that provides tension in the filament. Figure reproduced from [25].

ture directly influences the evolution of the material parameter. For instance, a branch of a tree can be trained to grow in a certain shape (which makes for beautiful alleys in French garden). At first, the elastic structure is loaded and stressed into a particular shape. As time passes, the structure remodels itself in such a way as to relieve the stresses and the structure permanently sets in, even in the absence of loading.

As a simple example, consider the case of an unshearable, inextensible planar rod under end compression [21]. As the rod buckles it takes a new shape. At this point it is assumed that the natural state of the rod will evolve towards this equilibrium shape. That is, its intrinsic curvature $\hat{\kappa} = \hat{u}_2$ evolves in time towards its actual curvature. A simple model for viscoelastic relaxation of curvature is

$$T\frac{\partial \hat{\kappa}}{\partial t} = \kappa - \hat{\kappa} \tag{57}$$

where T is a typical time corresponding to the viscoelastic response of the material. The important point to notice here is that, after buckling, the curvature changes at all points and when the intrinsic curvature relaxes it takes different values at all point. The process depends on the loading and the parameters but also on the history of the loading process which makes it fundamentally different from the previous modeling (through parameter variation). To emphasize this point, consider Fig. 6 where an initially straight rod was loaded with a given ramp and allowed to relax following the rule given.

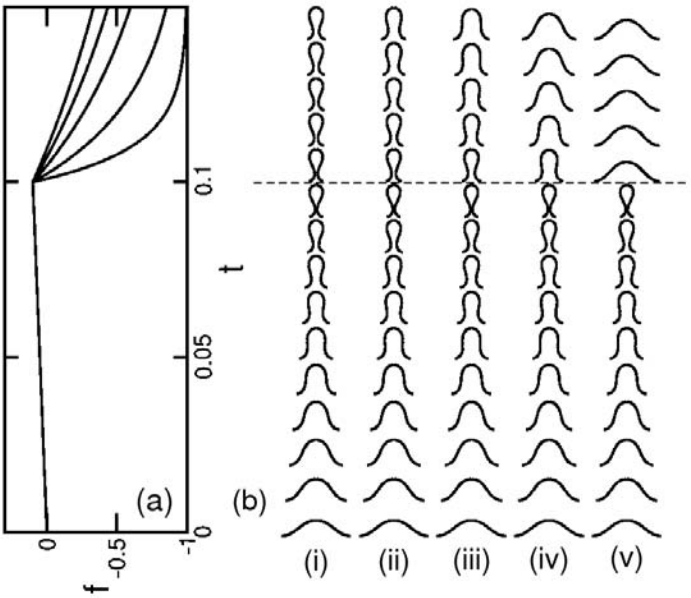

Fig. 6. Filaments trained with time-dependent forces. For each of the force-time profiles shown in (a) is the corresponding sequence of filament shapes (a) shown at intervals of $\Delta t = 0.01$. Dashed line indicates end of linear ramp [21]. As can be clearly seen in picture (i), the filament has remodeled into its shape and retains it after the load is removed. With longer unloading times ((ii) to (v)), the filament when unloaded, partially relaxes to its original shape.

Growing Rods: Evolution of the Natural Configuration

The two previous modeling approaches work for systems where the law for the growth evolution of the material can be described by changes in the material parameters. However, it is not suitable to describe other aspects of growth. For instance, consider a naturally straight untwisted rod in its unstressed configuration and allow it to increase in length. If the increase in length is uniform (independent of the material parameter), then it can be described by changing the length (a material parameter) as before. However, if growth is not uniform but depends on the position, stresses, or strains, the growth evolution cannot be simply described by a change in the material parameters. The essence of the problem comes from the fact that the reference configuration of the rod changes due to growth. For the purpose of this discussion consider an unshearable but extensible rod assume that growth only acts by changing the local element of length. The strain variable associated with a local change in length is $\mathsf{v}_3 = \lambda$. If the rod is not growing, a typical constitutive law for $\lambda = \lambda_\mathrm{e}$ is

$$\mathsf{n}_3 = \epsilon(\lambda_\mathrm{e} - 1) \tag{58}$$

with an extension modulus ϵ relating the tension in the rod to its elastic extension ($\lambda_e > 1$) or compression ($0 < \lambda_e < 1$). Now, the extension may also be created through growth. In the absence of tension, we introduce λ_g to describe the local extensional growth ($\lambda_g > 1$ for growth). In general when both growth and elasticity are combined, we split the extensional strain into

$$\lambda = \lambda_e \lambda_g \tag{59}$$

Since we have introduced a new strain variable λ_g a constitutive relationship for its evolution must be prescribed. This depends on the system being considered (see Section 4.1 for a discussion). Typically, an equation for the evolution of the growth rate as a function of the stress and material parameter will be specified

$$\dot{\lambda}_g = \lambda_g F(\mathbf{n}, s). \tag{60}$$

As an example of a local growth law, we consider the evolution of length and twist in a model for the growth of *Bacillus subtilis*.

3.5 Application to the Growth of Bacillus subtilis

The individual cells of the bacterial strain *Bacillus subtilis* are rod-shaped and typically of length $3 - 4\mu m$ and diameter $0.8\mu m$. Under certain circumstances they are found to grow into filaments consisting of the cells linked in tandem due to the failure of daughter cells, produced by growth and septation, to separate. As they elongate these filaments, which are immersed in a liquid environment (whose temperature and viscosity can be controlled), are observed to twist at uniform rate. The degree of twist and handedness can, in fact, be controlled experimentally and a wide range of states from left-handed to right-handed forms, can be produced. The actual twist state of the cells seems to be related to properties of the polymers which are inserted into the the cell wall during growth. As they elongate the filaments are observed to writhe and eventually deform into double-helical structures. These continue to grow and periodic repetition of this process results in macroscopic fibers (termed "macro-fibers") with a specific twist state and handedness. (A schematic representation of this dynamics is given in Fig. 7).

A striking feature of this iterated process is that at every stage of the self-assembly, the handedness of the helical structures that are created is the *same* (e.g. a right-handed double helix gives rise to a right-handed four-strand helix and so on). The nature of the environment does, however, influence certain aspects of the self-assembly. In a viscous environment the basic writhing instability leads to something of a "buckling" at the middle of the filament with the formation of a tight central loop; this is followed by a helical wind-up which starts at the base of this loop (Fig. 7B). By contrast, in a non-viscous medium, the instability causes the filament to fold over into a large loop closed by contact between the ends of the filament. This closure is then followed by

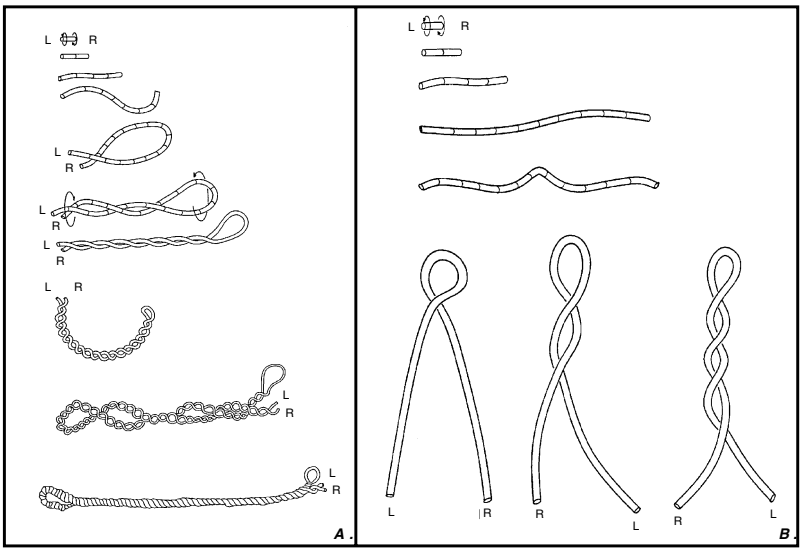

Fig. 7. The two basic looping of *Bacillus subtilis*: A. In non-viscous medium, B. In viscous medium (Picture courtesy of Neil Mendelson).

a helical wind-up starting at that point. In both cases this self-assembly conserves handedness and usually continues over long periods until macro-fibers, several millimeters long, are formed.

The dynamics of the self-assembly and the mechanical properties of the bacterial threads have been studied in great detail by Mendelson and coworkers over many years [51–53]. In addition to the fascinating questions of growth and form raised by this process, the macrofibers themselves offer the prospect of unusual bio-materials that can be mineralized and packed in ways that are are of practical biomedical and biotechnical use.

Mathematical modeling of Bacillus subtilis presents many challenges. With a little thought the handedness preserving nature of the basic instability can be explained in qualitative terms in which an "under-twisted" filament undergoes a writhing instability. Fundamental to this picture is the idea of an "intrinsic twist" associated with each cell and which drives the dynamics. This picture is, in a sense, quite universal and can also be seen in other filamentary structures ranging from the microscopic (e.g. DNA) to the macroscopic (*e.g.* telephone cables). The case of *Bacillus subtilis* is complicated by the fact that the cell filament is growing exponentially and that the ends of the filament are normally unconstrained. This freedom of the ends is a nontrivial feature of the basic instability that initiates the self-assembly. Once the filament has folded over (in either a big loop for non-viscous media or a tight central loop for viscous ones) the resulting self-contact effectively blocks free rotation of the filament. This changing of boundary conditions (one end is now effec-

tively fixed) provides the mechanism for the subsequent helical wind up of the strands.

In *Bacillus subtilis* (and DNA) where the twisting and supercoiling are of the *same* handedness. The key to this transition is the idea of an *intrinsic twist*; namely a natural state of the filament with a non-zero twist density (twist per unit length) as described in the Kirchhoff model by Eq.(52) with a non-vanishing parameter $\hat{u}_3$.

To understand the process, consider a rubber tube with right-handed intrinsic twist represented by drawing marker lines with a right-handed helical pitch. One end is twisted in the opposite direction to the marker lines until they are approximately straight. The twist density of the filament now appears to be zero whereas its natural state is one of non-zero twist density - as indicated by the original helical marker lines. Thus we now have a "twist deficit". To return to its natural state the tube must make up for this deficit by restoring twist. This can be achieved in two different ways. If one end is freed the tube winds sending a twist wave down the rod. Alternatively, if the ends are held but brought towards each other, the tube will relax by supercoiling with the *same* handedness as the intrinsic twist. This is the behavior observed in *Bacillus subtilis* and DNA. In the latter case the "intrinsic" twist corresponds to the right-handed helical architecture and in the former it is believed to be related to either the cell wall architecture or anisotropy.

In order to model *Bacillus subtilis* each bacterial cell is assumed to possess an "intrinsic" twist and to make up part of an elastic filament. Reproductive growth of all the cells in the bacterial filament results in an exponential growth of its length accompanied by a reduction of twist density.

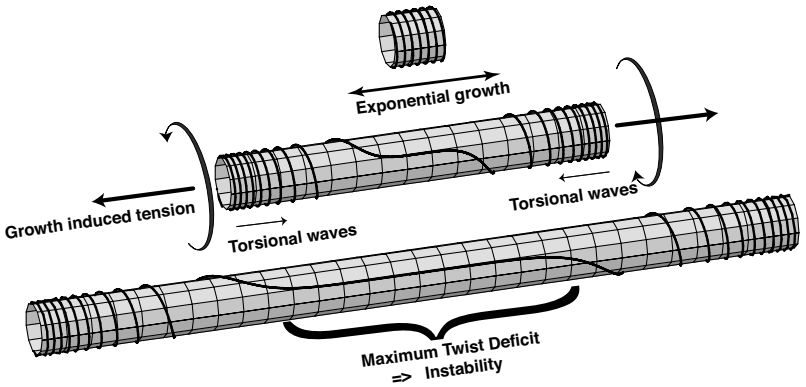

Fig. 8. Exponential growth and linear torsional wave competition, as the filament growth exponentially, the linear twist wave propagating from the end do not reach the middle of the filament where the twist deficit is maximal.

Using Kirchhoff's model as a starting point, we can study the dynamical properties of filaments and generalize it, as explained in the previous section, to include the effect of growth. Mathematical results on the stability of thin elastic rods [27] have enabled us to develop a complete picture of the mechanism of self-assembly in *Bacillus subtilis* [26] as well as computer simulation [41, 42]. Among other things the model gives quantitative predictions about the self-assembly geometry, such as the way the loop size scales with environmental conditions. The computer simulation of growing rod with intrinsic twist predicts the formation of looping in filaments remarkably similar to the ones found in the experiments (See Fig. 9)

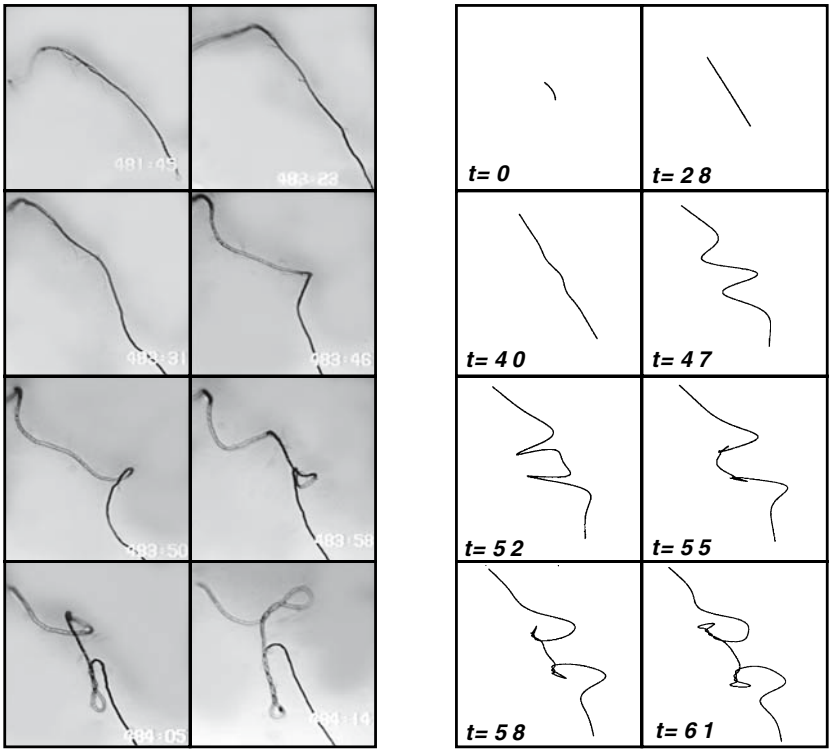

Fig. 9. Writhing Dynamics of *B. subtillis*. Left: experiments (Courtesy of Neil Mendelson), Right: Simulation of Kirchhoff rods with growth [41, 42].

A great deal of experimentation has shown that the twist state and helix hand of *B. Subtillis* macrofibers stem from the individual cell from which the fiber is derived. The information required to control macrofiber morphogenesis appears to reside in the growth plan of this cell and all its descendants. Intrinsic twist, a key feature of the dynamic model described here, is a logical

candidate for the mechanical information in the growth plan that dictates all subsequent growth and form.

Although our discussion here has focussed on the behavior of *B. subtillis*, filamentary structures are common in biological materials encompassing scales from molecular to organismal and we believe that the types of arguments forwarded here; namely the importance of axial growth, the decomposition of strain variables, buckling instability, twist-to-writhe conversion as a dynamical process and the special role played by intrinsic twist (or, presumably in other contexts, intrinsic curvature), may have quite general applicability.

4 Three-dimensional Growth

We now turn our attention to a general formulation of growth for three-dimensional nonlinear elastic body.

4.1 Basic Definitions of Morphoelasticity

Consider a continuous body with *reference configuration* $\mathcal{B}_0$. Let $\mathbf{X}$ denote the position vectors in $\mathcal{B}_0$. Now suppose the body is deformed to a new configuration, $\mathcal{B}_1$. We refer to $\mathcal{B}_1$ as the *current configuration* where the body is defined by $\mathbf{x} = \boldsymbol{\chi}(\mathbf{X}, t)$. The deformation gradient, $\mathbf{F}$(X,t)=Grad $\boldsymbol{\chi}$, relates a material segment in the reference configuration to the same segment in the current configuration. The key idea[2]introduced by Rodriguez, Hoger, and McCulloch [60] is to decompose the total deformation into a growth tensor $\mathbf{G}$(X,t) and an elastic tensor $\mathbf{A}$(X,t)

$$\mathbf{F}(\mathbf{X}, t) = \mathbf{A}(\mathbf{X}, t) \cdot \mathbf{G}(\mathbf{X}, t). \tag{61}$$

That is, the growth deformation may not result in a continuous change from point to point and may not be compatible. However, if we require continuity as the body grows, then an elastic deformation is introduced to maintain compatibility. As shown in Fig. 10, the growth tensor $\mathbf{G}$(X,t) maps $\mathcal{B}_0$ to the virtual configuration V_1 which is locally stress-free. The elastic deformation then maps V_1 to a grown stressed state $\mathcal{B}_1$ in order to maintain continuity of the body. The overall deformation gradient is the composition. Because of the need to ensure compatibility, the elastic deformation is introduced which in turn causes residual stress in the body.

[2] We also note that this decomposition was earlier introduced by Lee [44] who proposed representing elasto-plastic deformations in the form $\mathbf{F} = \mathbf{F}_e\mathbf{F}_p$, where $\mathbf{F}_e$ denotes the contribution to the total deformation as a result of elastic deformation, and $\mathbf{F}_p$ denotes the contribution to the total deformation due to plastic deformation. This has become a classical tool of elasto-plasticity. Note however, that there are still fundamental problems associated with such multiplicative decomposition (see for instance [55] or [77]).

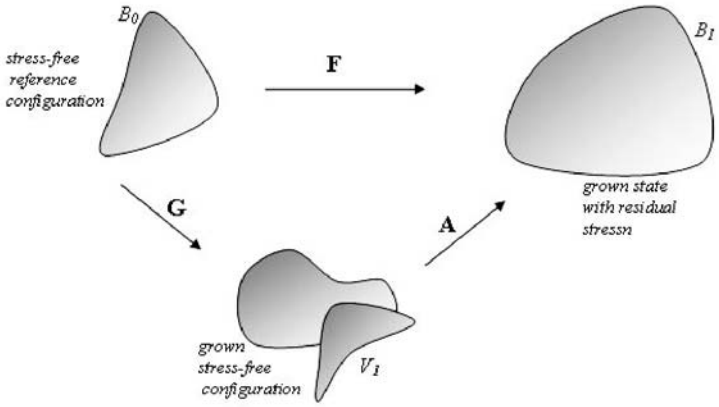

Fig. 10. The decomposition of finite growth. The deformation gradient $\mathbf{F}$ maps the reference configuration $B_0(\mathbf{X},t)$ into the current configuration $\mathcal{B}_1$. $\mathbf{F}$ can be represented as the product of a growth tensor $\mathbf{G}$ and an elastic deformation tensor $\mathbf{A}$. The intermediate configuration V_1 is a virtual state because $\mathbf{G}$ may not maintain continuity.

4.2 Strain Rate

We first recap some of the standard formalism and terminology. The tensor $\mathbf{F}$ is the *deformation gradient*, and

$$\mathbf{E} = \frac{1}{2}(\mathbf{F}^T\mathbf{F} - I), \tag{62}$$

is the Green (Lagrangian) strain tensor, and

$$\mathbf{D} = \mathbf{A} - I, \tag{63}$$

is the *displacement gradient*. Thus

$$\mathbf{E} = \frac{1}{2}(\mathbf{D} + \mathbf{D}^T + \mathbf{D}^T\mathbf{D}). \tag{64}$$

The linearization of this, $\mathbf{E} = \frac{1}{2}(\mathbf{D} + \mathbf{D}^T)$ is, of course, the familiar strain tensor of linear elasticity theory. If $\dot{(\,)}$ denotes differentiation w.r.t. time for fixed reference coordinate values, X, then one may show that the *rate of deformation*

$$\dot{\mathbf{F}} = \boldsymbol{\Gamma}\mathbf{F}, \tag{65}$$

where

$$\boldsymbol{\Gamma} = \operatorname{grad}\mathbf{v}(x,t), \tag{66}$$

is the Eulerian velocity gradient tensor, and hence

$$\dot{\mathbf{E}} = \mathbf{F}^T \Sigma \mathbf{F}, \tag{67}$$

where

$$\boldsymbol{\Sigma} = \frac{1}{2}(\boldsymbol{\Gamma} + \boldsymbol{\Gamma}^T), \tag{68}$$

is the *Eulerian strain rate tensor* [56]. Because $\boldsymbol{\Sigma} = \mathbf{F}^{-T}\dot{\mathbf{E}}\mathbf{F}^{-1}$ it is not a direct time derivative of $\mathbf{E}$, and thus cannot be called a (true) *rate of strain* tensor. However to first order

$$\dot{\mathbf{E}} = \mathbf{A}^T \boldsymbol{\Sigma} \mathbf{F} \simeq (I + \mathbf{D})^T \boldsymbol{\Sigma}(I + \mathbf{D}) \simeq \boldsymbol{\Sigma} + \text{h.o.t}, \tag{69}$$

and thus, for the linear theory, we can call $\boldsymbol{\Sigma}$, a rate of strain tensor.

Equation(61) is the starting point for our own discussions of the combination of elasticity and growth in a three-dimensional setting. By analogy with elasto-plasticity, we will refer to this approach as the theory of *morphoelasticity*. It is worth recalling how it was originally introduced [60]. For a system with density, ρ, the rate of growth of mass per unit volume, V, is

$$\dot{m} = \frac{d(\rho V)}{dt}, \tag{70}$$

while by basic conservation

$$\dot{m} = \frac{\pi \rho}{\pi t} + \text{div}(\rho \mathbf{v}_g), \tag{71}$$

where v_g is the *growth velocity vector*. It should be noted that v_g is defined in the Eulerian frame. For constant density these two equations combine to give

$$\frac{dV}{dt} = \text{div}\mathbf{v} = Tr\mathbf{D}_g, \tag{72}$$

where $\mathbf{D}_g$ is the *rate of growth tensor* - which is analogous to the rate of deformation tensor in classical continuum mechanics. Since $\mathbf{D}_g$ is Eulerian it has the advantage of not requiring a reference configuration but, it can be related to a Lagrangian *rate of growth stretch tensor*, $\dot{U}_g$, through

$$\mathbf{D}_g = \frac{1}{2}\left(\dot{\mathbf{U}}_g \mathbf{U}_g^{-1} + U_g^{-1}\dot{\mathbf{U}}_g\right). \tag{73}$$

Since $\dot{\mathbf{U}}_g$ is Lagrangian, the actual growth stretch tensor $\mathbf{U}_g$ is simply given by

$$\mathbf{U}_g = \int^t \dot{\mathbf{U}}_g dt. \tag{74}$$

The growth stretch tensor $\mathbf{U}_g$ is related to the growth deformation gradient tensor G by the right polar decomposition

$$\mathbf{G} = \mathbf{R}_g \mathbf{U}_g. \tag{75}$$

A general argument is that, without loss of generality, one can set $\mathbf{R}_g = I$ and work with $\mathbf{G} = \mathbf{U}_g$. [3]

[3] It appears to us that the reason given by many authors about how the rotation part of $\mathbf{G}$ can always be absorbed in the rotational part of $\mathbf{F}$, and that $\mathbf{G}$

4.3 Cauchy Stress and Equations of Motion

The forces distributed on a body $\mathcal{B}_1$ include a contact-force density $\mathbf{t}_n$ and a body-force density $\mathbf{b}$. In accordance with Euler's laws of motion, the balance of linear momentum is written as

$$\int_{\mathcal{B}_1} \rho(\mathbf{x},t)\mathbf{b}(\mathbf{x},t)\mathrm{d}v + \int_{\partial\mathcal{B}_1} \mathbf{t}_n \mathrm{d}a = \int_{\mathcal{B}_1} \rho(\mathbf{x},t)\dot{\mathbf{v}}(\mathbf{x},t)\mathrm{d}v. \tag{76}$$

Cauchy's theorem states that if $\mathbf{t}_n$ is continuous in $\mathbf{x}$, then $\mathbf{t}_n$ depends linearly on the unit normal $\mathbf{n}$. In other words, there exists a linear transformation $\mathbf{T}$ independent of $\mathbf{n}$ such that

$$\mathbf{t}_n = \mathbf{T}\mathbf{n}, \tag{77}$$

where $\mathbf{T}$ is referred to as the Cauchy stress tensor. Using (77) and applying the divergence theorem to (76) leads to

$$\int_{\mathcal{B}_1} \left(\rho(\mathbf{x},t) + \mathrm{div}\mathbf{T} - \rho(\mathbf{x},t)\dot{\mathbf{v}}(\mathbf{x},t)\right) \mathrm{d}v = 0. \tag{78}$$

Equation (78) is valid for any body $\mathcal{B}_1$. This leads to Cauchy's first law of motion,

$$\mathrm{div}(\mathbf{T}) + \rho\mathbf{b} = \rho\dot{\mathbf{v}}. \tag{79}$$

If the body is at rest, that is $\mathbf{v}(\mathbf{x},\mathrm{t})=\mathbf{0}$ for all $\mathbf{x}\in\mathcal{B}_1$, the equilibrium equation becomes

$$\mathrm{div}(\mathbf{T}) + \rho\mathbf{b} = 0. \tag{80}$$

Furthermore, if body forces are absent, (80) reduces to

$$\mathrm{div}(\mathbf{T}) = 0. \tag{81}$$

4.4 Strain-energy Functions

We assume that our material is hyperelastic. That is, there exists a strain-energy function $W = W(\mathbf{F})$ from which the stresses can be derived.

$$\mathbf{T} = J^{-1}\mathbf{F}\frac{\partial W}{\partial \mathbf{F}} - p\mathbf{1}, \tag{82}$$

where $J = det(\mathbf{F})$ is equal to one in the incompressible case and p is a Lagrange multiplier associated with the internal constraint of incompressibility ($p = 0$ in the compressible case). Many different general functional forms have been proposed for the the response of elastic materials under loads [6,62,65]. Here, we show some typical functions that have been proposed to model either elastomers or soft tissues. For the sake of simplicity, we restrict our attention

needs to be diagonal to ensure objectivity is not satisfactory and requires further discussions–see [77].

to homogeneous isotropic materials. The energy can be written in terms of the principal stretches λ_1, λ_2, λ_3 (the square roots of the principal values of $\mathbf{F}^{\mathrm{T}}\mathbf{F}$) or, equivalently for incompressible solids, in terms of the first two principal invariants of the Cauchy-Green strain tensors,

$$I_1 = \lambda_1^2 + \lambda_2^2 + \lambda_3^2, \quad I_2 = \lambda_2^2\lambda_3^2 + \lambda_3^2\lambda_1^2 + \lambda_1^2\lambda_2^2. \tag{83}$$

An essential property of many biological material is the strain-stiffening property which can be modeled either by algebraic power dependence (one-term Ogden model), by exponential behavior (as in the popular Fung model), or by limited chain extensibility (Gent model [19, 35, 38]). These three models can be written with a single parameter (ν, α, β, respectively) such that the classical neo-Hookean model is obtained in the limits $\nu \to 2$, $\alpha \to 0$, or $\beta \to 0$. Additionally, we also use the classical Mooney-Rivlin strain-energy density, often used to model elastomers.

Name	Definition	soft tissues	elastomers
neo-Hookean	$W_{\mathrm{nh}} = \frac{1}{2}(I_1 - 3)$		
Mooney-Rivlin	$W_{\mathrm{mr}} = \frac{(I_1 - 3) + \mu(I_2 - 3)}{2(1+\mu)}$		
1-term Ogden	$W_{\mathrm{og}} = \frac{2(\lambda_1^\nu + \lambda_2^\nu + \lambda_3^\nu - 3)}{\nu^2}$	$\nu \geq 9$	$\nu \approx 3$
Fung	$W_{\mathrm{fu}} = \frac{\exp \alpha(I_1 - 3) - 1}{\alpha}$	$3 < \alpha < 20$	
Gent	$W_{\mathrm{ge}} = \frac{-\log[1 - \beta(I_1 - 3)]}{\beta}$	$0.4 < \beta < 3$	$\beta < 0.05$

Table 1. A list of strain-energy functions. Note that the materials share the same infinitesimal shear modulus, which without loss of generality was taken equal to one. The limits $\mu \to 0$, $\alpha \to 0$, $\beta \to 0$, $\nu \to 2$ all lead to the neo-Hookean potential. References: 1-term Ogden [5, 66], Fung [13, 34] Gent [19, 20, 36, 37].

4.5 Constitutive Theory for G

There is an interesting discussion as to whether $\mathbf{G}$ or $\dot{\mathbf{G}} = \dot{\mathbf{U}}_g$ (the Lagrangian rate of growth tensor) can/should be a function of the Cauchy stress, namely

$$\mathbf{G} = f(\mathbf{T}), \quad \text{or} \quad \dot{\mathbf{G}} = g(\mathbf{T}). \tag{84}$$

Fung suggested that there might exist a growth equilibrium stress state $\bar{\mathbf{T}}$ at which the growth rate would be zero, *i.e.*

$$\dot{\mathbf{G}} = g(\mathbf{T} - \mathbf{R}\bar{\mathbf{T}}\mathbf{R}^T) \tag{85}$$

where the rotation tensor $\mathbf{R}$ comes from the polar decomposition and is required to ensure that both T and $\bar{T}$ are measured in the same frame of reference as required by objectivity.

There have been early on attempts to use the morphoelasticity formalism to model simple situations and understand the effect of growth and the feedback due to stress. These include the following cases:

Constant Growth

The simplest choice for $\mathbf{G}$ is to consider a constant tensor. A constant diagonal tensor $\mathbf{G}$ has been used in spherical geometry by Hoger and co-workers [9,43]. This case is interesting since analytical results can be obtained corresponding to small increments and explicit values of residual stress computed for growth without loading. In [4], the stability of such growing shells is considered.

Position Dependent Growth

Many growth processes depend on the location in the material. This effect is sometimes referred to as *differential growth* to indicate that some parts of a tissue grow faster than others. In morphoelasticity, it implies that $\mathbf{G}$ is a function of either $\mathbf{X}$ or $\mathbf{x}$. Both situations are of interest. In the first case, growth is a function of material points $\mathbf{X}$ in the reference configuration and this dependence assumes that the material is made out of points that grow at different rates and keep growing differentially as time goes by. In the second case, the ability of a tissue to grow depends on its location at any given time. This is the case, for instance, when cell reproduction depends on the availability of some nutrients that diffuse through the boundary. At any given time, the amount of nutrient may be described by the distance to the boundary as in the case in the growth of spheroids in tumor experiments [33]. The stability analysis of differentially growing shells was considered in [24].

Stress-dependence

It has been recognized experimentally and theoretically in many systems (such as aorta, muscles and bones) that one of the main biomechanical regulator of growth is stress [18,39,59,60,72–74]. It has even been suggested that stresses on cell walls play the role of a pacemaker for the collective regulation of tissue growth [67]. Accordingly, the growth rate tensor should be a function of the Cauchy stress tensor which could also vary according to the position of tissue elements in the reference configuration.

Most growth laws are of a phenomenological nature (See however the discussion in [18]) and currently there is no established theory of how they can be derived from biophysical principles An intriguing contribution appeared in [14] where it is assumed that growth can be associated with mechanical

accretive forces. In this context, the energy stored in the growth process can be transformed into mechanical elastic energy. By neglecting the possibility of energy sources and under suitable assumptions, a dissipation principle for the growth law can be derived, which in turn leads to a constitutive equation for the growth rate

$$\mathbf{G}^{-1}.\dot{\mathbf{G}} = \mathbf{M}_0 - W\mathbf{I} + A^T W_{\mathbf{A}} \tag{86}$$

where, as before, W is the free energy. We note that $W\mathbf{I} - A^T W_{\mathbf{A}}$ has the form of an Eshelby tensor as found in the theory of elasto-plasticity [15,49], and that for small deformations, $\mathbf{M}_0$ plays the role of a constant (homeostatic) stress. These constitutive relations (shown here in the simplest case) are typically nonlinear and deserve further exploration.

4.6 Cumulative Growth

Now consider a sequence of growth steps in which each step can be decomposed into a growth deformation and an elastic deformation (see Fig. 11).

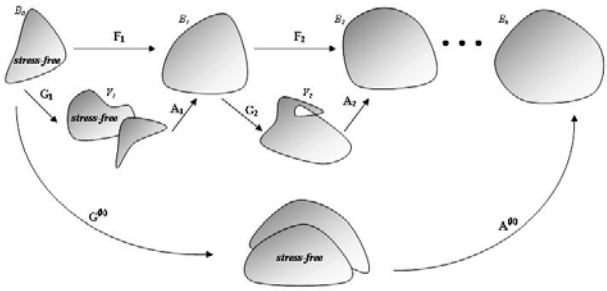

Fig. 11. Cumulative growth with k steps.

The cumulative deformation gradient is given by

$$\begin{aligned}\mathbf{F}^{(k)} &= \mathbf{F}_k \cdot \mathbf{F}_{k-1} ... \mathbf{F}_2 \cdot \mathbf{F}_1 \\ &= \mathbf{A}_k \cdot \mathbf{G}_k \cdot \mathbf{A}_{k-1} \cdot \mathbf{G}_{k-1} ... \mathbf{A}_2 \cdot \mathbf{G}_2 \cdot \mathbf{A}_1 \cdot \mathbf{G}_1.\end{aligned}$$

Assume the growth and elastic tensor commute, that is $\mathbf{A}_i \cdot \mathbf{G}_j = \mathbf{G}_j \cdot \mathbf{A}_i$, for all i, j. Then the elastic and growth tensors can be written as

$$\mathbf{A}^{(k)} = \mathbf{A}_k \cdot \mathbf{A}_{k-1} ... \mathbf{A}_2 \cdot \mathbf{A}_1, \qquad \mathbf{G}^{(k)} = \mathbf{G}_k \cdot \mathbf{G}_{k-1} ... \mathbf{G}_2 \cdot \mathbf{G}_1. \tag{87}$$

The stress in $\mathcal{B}_k$ is

$$\nabla_{x_k} \cdot (\mathbf{T}_k) = 0, \tag{88}$$

where

$$\mathbf{T}_k = \mathbf{A}^{(k)} \cdot \partial_{\mathbf{A}^{(k)}} W - p_k \mathbf{1}. \tag{89}$$

An example of a cumulative process of growth is given in Section 4.9.

4.7 A Simple Example of Homogeneous Growth

As a first example, we revisit the model of Rodriguez, *et al.* [60] where growth is a function of the stress tensor. Because the problem is homogeneous, residual stress is absent. A rectangular block of bone is subjected to compression along its longitudinal axis. It grows along the x and y directions as a linear function of the difference between the axial stress and a no-growth equilibrium stress state. The bone is assumed to have a Young's modulus of 18.4 GPa along the z-axis. According to the authors "...at each step the axial strain is adjusted so that the applied axial *force* remains constant." Recalling that stress = force/area, the calculation proceeds as follows. At each step the cross sectional area $S(t) = A_{xx}(t)A_{yy}(t) = \lambda_{xx}(t)\lambda_{xx}(t)/\lambda_z(t)$ is computed. In order to ensure that the axial force, $F = T_{zz}(t)S(t)$, where T_{zz} is a certain function of λ_z, remains constant, λ_z is reduced as necessary. This, in turn, reduces T_{zz} at the next step until it reaches $\bar{T}_{zz}$ at which point the computation stops. In this model the stresses are only as a result of loading so there is no residual stress.

More explicitly, the reference configuration is compressed along the longitudinal axis which results in the elastic deformation gradient

$$A = \mathrm{diag}\left(\frac{1}{\sqrt{\lambda_z}}, \frac{1}{\sqrt{\lambda_z}}, \lambda_z\right), \tag{90}$$

where λ_z is the stretch ratio corresponding to a 0.1% shortening ($\lambda_z = 0.999$). The strain is calculated from the Green strain tensor

$$\mathbf{E} = \frac{1}{2}(\mathbf{A}^T\mathbf{A} - \mathbf{I}), \tag{91}$$

and the longitudinal stress is found from

$$\mathbf{T} = \mathbf{A}^T\frac{\partial W}{\partial \mathbf{E}}\mathbf{A}, \tag{92}$$

where the strain energy is given by

$$W = c_1(E_{xx}^2 + E_{yy}^2 + E_{zz}^2). \tag{93}$$

The stress along the z-direction is then

$$\begin{aligned} t_3 &= 2c_1E_{zz}F_{zz}E_{zz} \\ &= c_1\lambda_z^2(\lambda_z^2 - 1), \end{aligned}$$

where $2c_1$ is the value of the Young's modulus along the z-direction. Following the elastic deformation, the tissue grows or resorbs along the x and y axes until equilibrium is restored. The equilibrium value for the longitudinal stress is given by t_3^*. The rate of growth in the x and y directions at time t is given by

$$\lambda_x(t) = k_x(t_3(t) - t_3^*), \tag{94}$$

$$\lambda_y(t) = k_y(t_3(t) - t_3^*), \tag{95}$$

where k_x and k_y are growth rate constants with equal values of -0.27 time^{-1}GPa^{-1} and the no-growth equilibrium longitudinal stress t_3^* is -4.5 MPa. The growth stretch ratios with respect to the reference configuration can be written as

$$\lambda_x(t + \mathrm{d}t) = \lambda_x(t) + \dot{\lambda}_x \mathrm{d}t, \tag{96}$$

$$\lambda_y(t + \mathrm{d}t) = \lambda_y(t) + \dot{\lambda}_y \mathrm{d}t, \tag{97}$$

where dt corresponds to one iteration. The growth deformation gradient is then

$$\mathbf{G}(t + \mathrm{d}t) = \mathrm{diag}\left(k_x(t_3(t) - t_3^*)\mathrm{d}t + G_{xx}(t), k_y(t_3(t) - t_3^*)\mathrm{d}t + G_{yy}(t), G_{zz}\right). \tag{98}$$

The axial stress is computed after each iteration and the tissue growth is then calculated. The applied axial load remains constant through each iteration and the axial stress is adjusted in order to maintain this force. Each growth deformation is assumed to be compatible and therefore no residual stress arises. Fig. 12 shows the axial stress and the growth stretch ratios (λ_x and λ_y) as functions of time. Following each iteration, the cross-sectional area increases which causes a decrease in the elastic stress and a decrease in the growth rate.

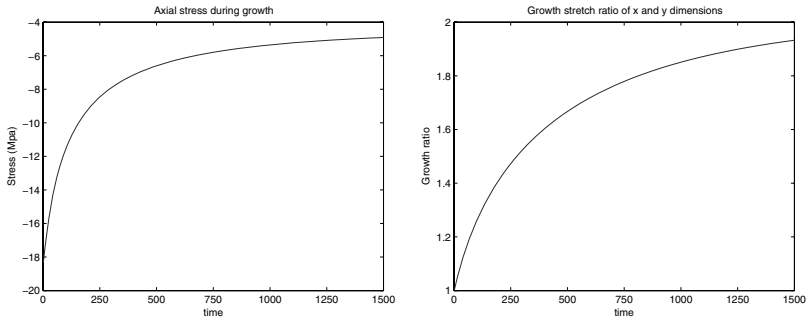

Fig. 12. A load leading to a 0.1% shortening on a block of bone is imposed. The block grows as a linear function of the difference between the loading stress and the no-growth equilibrium stress state. The left panel shows the axial stress as a function of time as it approaches the no-growth equilibrium stress. The right panel displays the growth ratios for the x and y directions.

The evolution of the axial stress can be written as a discrete mapping given by

$$t_3(t+\mathrm{d}t) = \frac{t_3(0)}{\left(\sqrt{\frac{t_3(0)}{t_3(t)}} + k_x(t_3(t) - t_3^*)\right)^2}. \tag{99}$$

The mapping can be converted to the following differential equation:

$$\frac{\mathrm{d}t_3(t)}{\mathrm{d}t} = \frac{t_3(0)t_3(t)}{\left(\sqrt{t_3(0)} + k_x\sqrt{t_3(t)}(t_3(t) - t_3^*)\right)^2} - t_3(t). \tag{100}$$

Fig. 13 shows the discrete mapping presented by Rodriguez *et al.*, as well as the numerical solution to Equation (100).

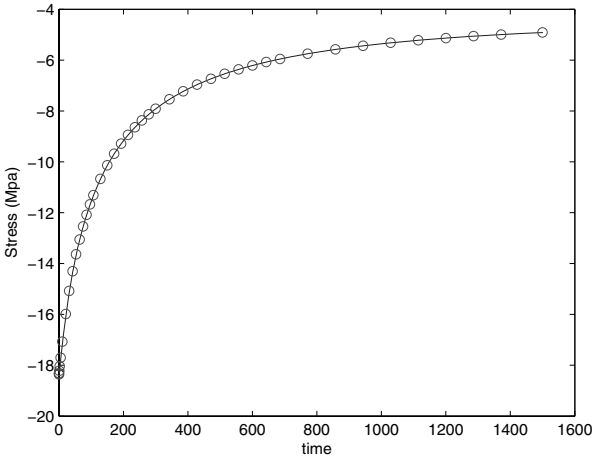

Fig. 13. Comparison between the continuous solution (solid curve) and the discrete solution (open circle) obtained by incremental computation.

To supplement the previous results, consider stress-dependent growth in the case of a cylindrical tube. The tube is initially subjected to compression along its longitudinal axis resulting in a 0.1% shortening ($\lambda_z = 0.999$). An elastic energy associated with a Neo-Hookean material is used. After axial compression, the cylinder is allowed to grow in which the following stress dependent growth deformation gradient is used:

$$\mathbf{G}(t+\mathrm{d}t) = \mathrm{diag}\left(k(t_3(t) - t_3^*)\mathrm{d}t + G_{rr}(t), k(t_3(t) - t_3^*)\mathrm{d}t + G_{\theta\theta}(t), G_{zz}\right). \tag{101}$$

where $k = -0.27\ \mathrm{time}^{-1}\mathrm{GPa}^{-1}$ and $t_3^* = -4.5$ MPa.

In the cylindrical case, the material response is not homogenous, and therefore the longitudinal force is now a function of the radial component. Therefore, consider the resultant load, $N = \int_a^b rt_3(r)dr$, and the resultant

longitudinal force $F_z = N \cdot Area$. In each iteration, the resultant axial stress is evaluated and the material is allowed to grow. The applied resultant axial force F_z is constant at each step and the the resultant longitudinal stress is adjusted accordingly to maintain the constant force. Fig. 14 shows the resultant axial stress as a function of time. The curve is approaching the equilibrium resultant stress, $N^* = \int_a^b rt_3^* dr$.

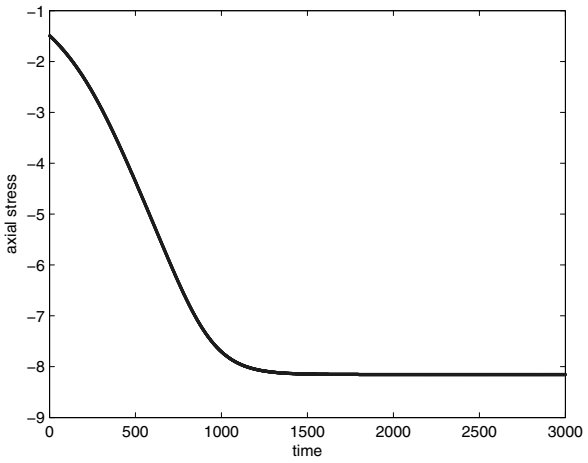

Fig. 14. Resultant longitudinal stress for an axially loaded cylinder. An initial five percent shortening was incurred. The cylinder was allowed to grow as the state of stress goes toward the predetermined equilibrium state.

We comment that the convenient thing about doing the calculation in discrete time steps is that one does not have to worry about separating elastic and growth time scales: one simply makes whatever elastic adjustments are necessary before implementing the next growth step.

4.8 Cylinder Growth: One Step Growth

We now consider a simple growth tensor to demonstrate how residual stress can arise from growth. Consider a cylindrical tube whose reference configuration has length L and internal and external radii A and B respectively. Therefore the tube is defined as

$$A \leq R \leq B, \qquad 0 \leq \Theta \leq 2\pi, \qquad 0 \leq Z \leq L. \tag{102}$$

Now let the cylinder undergo uniform circumferential growth or resorption which then results in an elastic deformation. The resulting deformation is given by

$$r = r(R), \qquad \theta = k\Theta, \qquad z = \lambda_z Z. \tag{103}$$

The deformation gradient in cylindrical coordinates is

$$\mathbf{F} = \mathrm{diag}(r', \frac{r}{R}, \lambda_z) \tag{104}$$

where $r' = \frac{dr}{dR}$. Assume there is no change in length so that $\lambda_z = 1$. The deformation tensor is decomposed as $\mathbf{F} = \mathbf{A}\cdot\mathbf{G}$. Assuming constant circumferential growth, the growth deformation gradient is

$$\mathbf{G} = \mathrm{diag}(1, k, 1), \tag{105}$$

where $\mathbf{G}$ maps the reference state $\mathcal{B}_0$ into the grown stress-free state V. In order to maintain continuity of the body, an elastic deformation

$$\mathbf{A} = \mathrm{diag}(\frac{1}{\alpha}, \alpha, 1), \tag{106}$$

maps the virtual stress-free state V to the final intact configuration $\mathcal{B}_1$. Note the incompressibility condition $\det\mathbf{A} = 1$ is used to express the three principal strain components in terms of a single variable α. Assuming the cylindrical tube is composed of a Fung material, the strain energy function is

$$W_{\mathrm{fu}} = \frac{c}{2}(e^Q - 1), \tag{107}$$

where c is a constant and Q is a function of the three principal strain values, that is $Q = 2b_1(\lambda_1^2 + \lambda_2^3 + \lambda_3^2)$. In the present case $\lambda_1 = 1/\alpha, \lambda_2 = \alpha$, and $\lambda_3 = 1$. Therefore, Q is given by

$$Q = 2b_2(\frac{1}{\alpha^2} + \alpha^2 - 2). \tag{108}$$

The incompressibility constraint is $\det(\mathbf{A}) = 1$, or equivalently $\det(\mathbf{F}\mathbf{G}^{-1}) = 1$. This implies $\det(\mathbf{F}) = \det\mathbf{G}$, so that

$$\frac{r'r}{R} = k. \tag{109}$$

The previous equation can be integrated to obtain

$$r = (a^2 + k(R^2 - A^2))^{1/2}. \tag{110}$$

The incompressibility constraint along with the relation $\mathbf{F} = \mathbf{A}\mathbf{G}$ provides an equation for the strain, $\alpha = r/(kR)$. The only non-vanishing equilibrium equation in (81) is

$$\frac{\partial t_1}{\partial r} + \frac{t_1 - t_2}{r} = 0. \tag{111}$$

The radial stress and hoop stress are denoted as $t_1 = T_{11}$ and $t_2 = T_{22}$, respectively. Using the stress-strain relationship in Equation (82), equations for the radial and hoop stress can be written as

$$t_1 = \frac{1}{\alpha}\frac{\partial W}{\partial \lambda_1} - p \tag{112}$$

$$t_2 = \alpha\frac{\partial W}{\partial \lambda_2} - p. \tag{113}$$

Substitute these values into (111) to obtain a closed equation for t_1:

$$\frac{\partial t_1}{\partial r} = \frac{\alpha}{r}\partial_\alpha \hat{W} \tag{114}$$

where $\hat{W} = W(\frac{1}{\alpha}, \alpha, 1)$. In terms of R,

$$\frac{\partial t_1}{\partial R} = \frac{\partial_\alpha \hat{W}}{k\alpha R}. \tag{115}$$

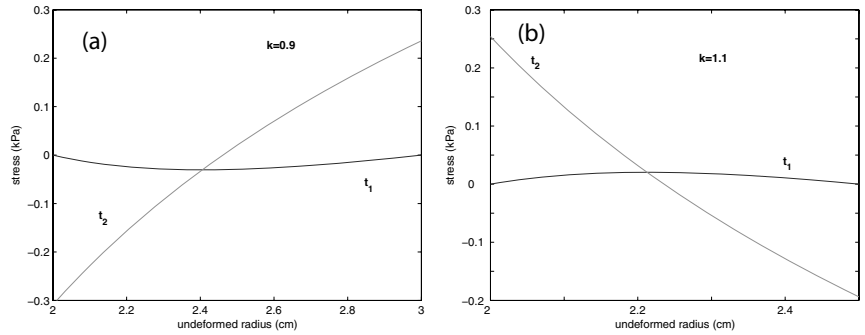

Fig. 15. Plots of residual stress vs. undeformed radius for a cylindrical tube following uniform circumferential resorption (a) and growth (b). The cylinder is unload which results in zero radial stress at the boundaries in both cases. When k=0.9 (resorption) the circumferential residual stress is in compression in the inner wall and in tension in the outer wall. When k=1.1 (growth) the circumferential residual stress is tensile in the inner layers and compressive in the outer layers.

Using the boundary conditions $t_1(A) = t_1(B) = 0$, integrate the last equation to obtain an equation for the radial stress

$$t_1(R) = \frac{1}{k}\int_A^R \frac{\partial_\alpha \hat{W}}{\alpha R} dR, \tag{116}$$

and now the hoop stress can be evaluated as $t_2 = t_1 + \frac{\alpha}{2}\partial_\alpha \hat{W}$. The hollow cylindrical tube model demonstrates how circumferential growth produces a transmural distribution of residual stress that would cause the cylinder to change shape when cut. Consider a tube with initial internal and external radii of 2.0 and 3.0 cm and $k = 0.9$ (resorption). Fig. 15(a) shows the radial

stress t_1 and the circumferential stress t_2. The radial stress is zero at the boundaries ($r = A$ and $r = B$) because the cylinder is unloaded. The circumferential stress is in compression in the inner layers and tension in the outer layers. The grown internal and external radii were 1.75 and 2.75 cm.

Now consider the growth case where $k = 1.1$. The equilibrium internal and external radii were 2.25 and 3.25 cm. Notice in Fig. 15(b) the graphs are reversed from the resorption case. The circumferential stress is in tension in the inner layers and compression in the outer layers. The longitudinal stress t_3 is nonzero in both the resorption and growth cases. The longitudinal stress will cause the cylinder to extend or shorten. However, the resultant stress is close to zero, and therefore the simplifying assumption of $\lambda_z = 1$ will not affect the circumferential residual stress. In the three-dimensional problem, we will later discuss how to circumvent the issue of a non-zero longitudinal stress on the ends of the cylinder.

4.9 Cylinder Growth: Modeling Incremental Growth

Consider once again a cylindrical tube but now assume the incremental growth tensor $\mathbf{G}_{inc}$ is a function of position. There is growth only along the z-axis, so that $\mathbf{G}_i = \text{diag}(1, 1, g(r_i))$. Because the incremental growth tensor is dependent on the current configuration, an implicit dependence on the stress tensor exists which must be computed at each iteration [23]. The growth function g_{inc} at the kth step along the z-axis is written as the product $g(R) = \prod_{i=1}^{k-1} g_{inc}(r_i)$ where r_i is the current configuration following the i-th deformation. The cumulative deformation gradient in cylindrical coordinates after i steps is

$$\mathbf{F}_i = \text{diag}(r_i', \frac{r_i}{R}, \lambda_{z_i}), \tag{117}$$

where the cylinder is extended uniformly to length $l_i = \lambda_{z_i} l_{i-1}$. Denote the internal and external radii in the initial configuration by A and B, and let $a_i = r_i(A)$ and $b_i = r_i(B)$ be the radii in the current configuration. The principal stretches of the elastic tensor $\mathbf{A}$ are

$$\lambda_{i1} = g_i(R)(\alpha_i \lambda_{z_i})^{-1}, \qquad \lambda_{i2} = \alpha_i = \frac{r_i}{R}, \qquad \lambda_{i3} = \frac{\lambda_{z_i}}{g_i(R)}, \tag{118}$$

where α_i is defined as the azimuthal principal stretch. Assume the elastic cylindrical tube is composed of a neo-Hookean material, that is $W_{\text{nh}} = \mu(\lambda_{i1}^2 + \lambda_{i2}^2 + \lambda_{i3}^2 - 3)$. The incompressibility condition $\det(\mathbf{A}_i) = 1$ implies $\det(\mathbf{F}_i) = \det(\mathbf{G}_i)$ so that

$$\lambda_{z_i} \frac{r_i' r_i}{R} = g(R). \tag{119}$$

Integrate the last equation to find

$$r_i(R) = \left(a_i^2 + \frac{2}{\lambda_{z_i}} \int_A^R \rho g(\rho) d\rho \right)^{1/2}. \tag{120}$$

The constitutive relationships for t_1 and t_2 are as follows:

$$t_1 = \lambda_{i1} \frac{\partial W}{\partial \lambda_{i1}} - p, \tag{121}$$

$$t_2 = \lambda_{i2} \frac{\partial W}{\partial \lambda_{i2}} - p. \tag{122}$$

The only nonvanishing equilibrium equation of $\nabla_{x_i} \cdot (\mathbf{T}_1) = 0$ is, as previously shown in (111),

$$\frac{\partial t_1}{\partial r} + \frac{t_1 - t_2}{r} = 0. \tag{123}$$

Rearrange the previous equation and use (121) and (122) to obtain

$$\frac{\partial t_1}{\partial r_i} = \frac{\alpha_i}{r_i} \partial_\alpha \hat{W} \tag{124}$$

where $\hat{W} = W(\frac{g(R)}{\alpha \lambda_{z_i}}, \alpha, \frac{\lambda_{z_i}}{g(R)})$. In terms of R,

$$\frac{\partial t_1}{\partial R} = \frac{R g(R) \alpha_i}{\lambda_{z_i} r_i^2} \partial_{\alpha_i} \hat{W} \tag{125}$$

where (120) and (118) are used to express $r_i = r_i(R)$ and $\alpha_i = \alpha_i(R)$. We would like the surface of the cylinder to be free of any traction,

$$t_1(a_i) = t_1(b_i) = 0, \quad 0 \le \theta \le 2\pi, \quad 0 \le z_i \le \lambda_{z_i} l_{i-1}, \tag{126}$$

and

$$t_3(0) = t_3(\lambda_{z_i} l_{i-1}) = 0, \quad 0 \le \theta \le 2\pi, \quad a_i \le r_i \le b_i. \tag{127}$$

However, $t_3 = t_3(R)$ and does not explicitly depend on z_i. Therefore (127) requires $t_3 = 0$, but t_3 is a function of R and is not equal to zero. Instead, at each iteration we may solve for λ_{z_i} so that a zero resultant load N is imposed [17, 30–32]

$$N_i(\lambda_{z_i}) = 2\pi \int_{a_i}^{b_i} r_i t_3(r_i, \lambda_{z_i}) dr_i = 0. \tag{128}$$

Therefore, the end conditions in (127) are replaced by the condition above. Using (120), (125), and (126), the longitudinal stretch λ_{z_i}, the deformed radius a_i, and the radial stress t_1 can be found at each iteration and the deformation is completely determined. At each stage the growth function along the z-axis can be computed for the next iterate,

$$g(R) = \prod_{i=1}^{k} g_{inc}(r_i). \tag{129}$$

First consider a linear incremental growth function $g_{inc}(r_i) = 1 + \mu(r_i - a_i)$ where no longitudinal growth occurs at the inner wall and the growth linearly increases toward the outer wall. Choose initial values $A = 1$, $B = 2$, and calculate μ at each iteration such that the volume increases by 1%. Next consider the growth function $g_{inc}(r_i) = 1 + \mu(b_i - r_i)$ where no longitudinal growth occurs at the outer wall and the growth linearly increases toward the inner wall. Fig. 16 shows the cumulative growth function in the current configuration.

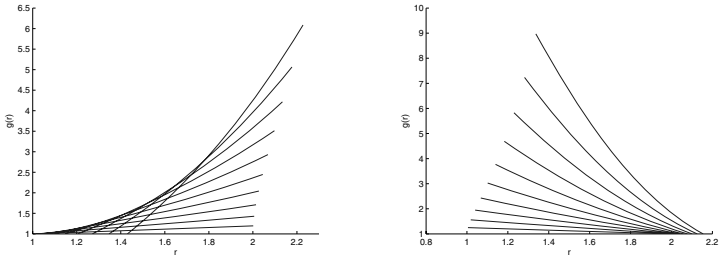

Fig. 16. The cumulative growth function viewed in the current frame $g = g(r)$. The volume increase in each step is 1%. The cumulative growth curve is plotted every ten steps.

Now consider changing μ and looking at how the longitudinal stress changes after one step. Fig. 17 shows $N(\lambda_z) = 2\pi \int_a^b r t_3(r, \lambda_z) dr$ as μ increases from zero to 1.5. In order to obtain a zero resultant load, we need to find $\lambda_{z_{crit}}$ such that $N(\lambda_z) = 0$. Once $\lambda_{z_{crit}}$ is found, Fig. 17 shows the longitudinal stress. When the inner layers of the cylinder grow faster than the outer layers, the inner layers are in compression and the outer layers are in tension as predicted. In contrast, when the outer layers of the cylinder grow faster than the inner layers, the inner layers are tensile and the outer layers are compressive.

4.10 Cylinder Growth: Embedded in an Elastic Medium

We can also nest two materials with different strain functions (i.e. a neo-Hookean material inside Fung material) or different growth factors. The boundary between the two materials, which we call C and c in the reference and current configurations respectively, is constrained so that no gaps form between materials.

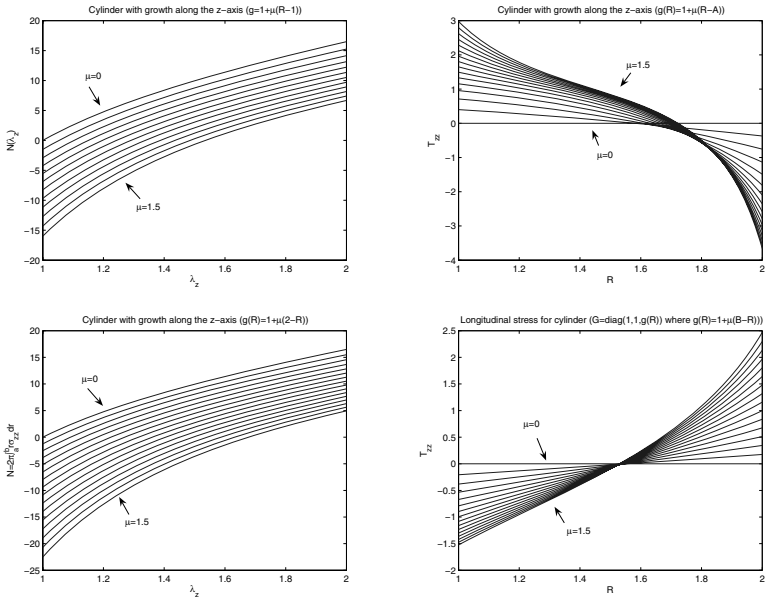

Fig. 17. Longitudinal stress along the cylinder radius (right). Note the compressive and tensile stress in different regions depending on which part of the cylinder grows faster.

As an example we look at two different materials. The inner material is neo-Hookean, and subject to shrinking in the radial direction ($\gamma_1 = 0.5$), while the outer material is Fung and is growing radially ($\gamma_1 = 2$). We set external pressure to zero, and set the initial boundary between the materials to halfway between the shell boundaries ($C = 1.5$).

Fig. 8 and Fig. 9 show the results for this configuration. As can be seen in the first figure, the deformation $r(R)$ is continuous, but the position of the boundary between layers is no longer halfway between the edges, rather it is closer to the inner deformed radius a. The second figure shows the stresses in the material due to growth, and there exist tensile and compressive stresses on all axes.

4.11 Cylinder Growth: with Twist

We now comment on growth models involving twist. The decomposition $\mathbf{F} = \mathbf{AG}$ is not unique and some thought needs to go into making a reasonable choice. Our model is that of a cylindrical rod that grows in length and exhibits growth induced twist, but maintains a constant radius. This would correspond to the (total) deformations

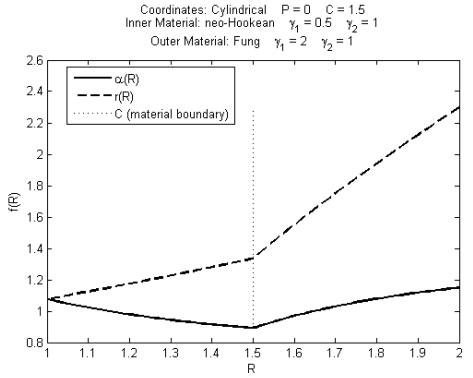

Fig. 18. The strain function $\alpha(R)$ and the deformation $r(R)$ for two nested materials (see text).

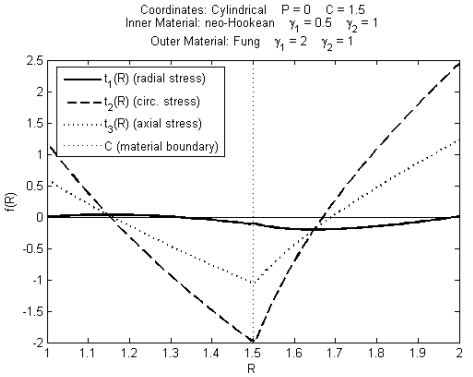

Fig. 19. The radial, circumferential and axial stresses for two nested materials (see text).

$$r = R \tag{130}$$

$$\theta = \Theta + z\tau = \Theta + \lambda Z\tau \tag{131}$$

$$z = \lambda Z. \tag{132}$$

Note that the torsion in the current configuration depends on the current height z. With these deformations, the (total) deformation gradient tensor is

$$\mathbf{A} = \begin{pmatrix} 1 & 0 & 0 \\ 0 & 1 & r\lambda\tau \\ 0 & 0 & \lambda \end{pmatrix}. \tag{133}$$

For our growth tensor we choose

$$\mathbf{G} = \begin{pmatrix} 1 & 0 & 0 \\ 0 & 1 & r\tau^* \\ 0 & 0 & \lambda \end{pmatrix}, \tag{134}$$

which corresponds to the growth-induced deformation

$$r = R \tag{135}$$
$$\theta = \Theta + Z\tau^* \tag{136}$$
$$z = \lambda Z, \tag{137}$$

where τ^* is a (fixed) twist determined by the growth process. Note that in the growth process we claim that the amount of torsion depends on the reference configuration height Z. The elastic deformation gradient tensor is easily determined to be

$$\mathbf{F} = \mathbf{A}\mathbf{G}^{-1} = \begin{pmatrix} 1 & 0 & 0 \\ 0 & 1 & r\left(\tau - \frac{\tau^*}{\lambda}\right) \\ 0 & 0 & 1 \end{pmatrix}. \tag{138}$$

With this form of $\mathbf{B}$, the Cauchy elastic stress tensor is

$$\mathbf{T}(\mathbf{F}) = \begin{pmatrix} T_{11} & 0 & 0 \\ 0 & T_{22} & T_{23} \\ 0 & T_{32} & T_{33} \end{pmatrix}, \tag{139}$$

where

$$T_{11} = P + \Phi + \Psi\left(2 + r^2\left(\tau - \frac{\tau^*}{\lambda}\right)^2\right) \tag{140}$$
$$T_{22} = P + \Phi + 2\Psi + (\Phi + \Psi)r^2\left(\tau - \frac{\tau^*}{\lambda}\right)^2 \tag{141}$$
$$T_{23} = (\Phi + \Psi)r\left(\tau - \frac{\tau^*}{\lambda}\right) \tag{142}$$
$$T_{32} = (\Phi + \Psi)r\left(\tau - \frac{\tau^*}{\lambda}\right) \tag{143}$$
$$T_{33} = P + \Phi + 2\Psi, \tag{144}$$

where P is the turgor pressure and $\Phi = 2\pi W/\pi I_1$, $\Psi = 2\pi W/\pi I_2$. For a Mooney-Rivlin material, Φ and Ψ are constant.

If we require that during growth the process is free of (residual) torsional stress, *i.e.* $T_{\theta z} = 0$, then the twist must obey

$$\tau = \frac{\tau^*}{\lambda}, \tag{145}$$

which also eliminates the elastic torsional strain, *i.e.* $\mathbf{F}_{\theta z} = 0$. If our growth model allows for (gradually) increasing length, *i.e.* λ increases with time, *then*

condition (145) shows that as the cylinder grows it gradually unwinds. Under this condition, all the other stress

$$T_{rr} = T_{\theta\theta} = T_{zz} = P + \Phi + 2\Psi, \tag{146}$$

only depend on the load (the turgor press P) and hence there is no residual stress at all.

5 Conclusions

In this article, we have reviewed different models to describe growth in biological systems. The common thread to most of these models is the decomposition of strain variables in elastic and growth components. The elastic component is connected to the stresses by the usual constitutive equation whereas the strain associated with growth requires a separate evolution law. These laws are not yet well-understood and much experimental and theoretical work is needed before a clear picture of how growth is related to stress emerges. Nevertheless, it is already possible to explore the consequences of growth such as the ability of a growing body to either build mechanical properties or undergo pattern formation through a buckling instability.

An area in which growth modeling will play an increasingly important role is in the modeling of tumor growth and cancer. We would just like to mention the existence of growing body of literature on various modeling aspects and data analysis of the problem that will drive the theory of growth (see [1, 3, 7, 8, 16, 33, 46, 54, 61, 63, 75]).

It is important to note that the description given here is not the only possible approach to modeling growth. Other interesting approaches to growth have been proposed either in terms of mixture theory, coupled with the evolution of natural configurations [40] or by focusing on the evolution of residual stress in the material [57].

Acknowledgement. This material is based upon work supported by the National Science Foundation under Grant No. DMS-0604704 (A. G.) and DMS-IGMS-0623989 (A.G. and M. T.). We are indebted to Martine Ben Amar for many interesting discussions and for her hospitality at the Ecole Normale Supérieure (Paris). This work was possible by the Centre National de la Recherche Scientifique (A. G. and M.T.).

References

1. D. Ambrosi and F. Mollica. The role of stress in the growth of a multicell spheroid. *J. Math. Biol.*, 48: 477–499, 2004.
2. S. S. Antman. *Nonlinear problems of elasticity.* Springer Verlag, New York, 1995.

3. R. P. Araujo and D. L. S. McElwain. New insights into vascular collapse and growth dynamics in solid tumors. *J. Theor. Biol.*, 228: 335–346, 2004.
4. M. Ben Amar and A. Goriely. Growth and instability in soft tissues. *J. Mech. Phys. Solids*, 53: 2284–2319, 2005.
5. D. K. Bogen and Th A. McMahon. Do cardiac aneurysms blow out? *Biophys. J.*, 27: 301–316, 1979.
6. M. C. Boyce and E. M. Arruda. Constitutive models for rubber elasticity: a review. *Rubber Chem. Technol.*, 73: 504–523, 2000.
7. H. Byrne and L. Preziosi. Modelling solid tumour growth using the theory of mixtures. *Math. Med. Biol.*, 20: 341–366, 2003.
8. C. Y. Chen, Byrne H. M., and J. R. King. The influence of growth-induced stress from the surrounding medium on the devlopment of multicell spheroids. *J. Math. Biol.*, 43: 191–220, 2001.
9. Y. Chen and A. Hoger. Constitutive functions of elastic materials in finite growth and deformation. *J. Elasticity*, 59: 175–193, 2000.
10. B. D. Coleman, E. H. Dill, M. Lembo, Z. Lu, and I. Tobias. On the dynamics of rods in the theory of Kirchhoff and Clebsch. *Arch. Rational Mech. Anal.*, 121: 339–359, 1993.
11. D. J. Cosgrove. Cell wall yield properties of growing tissue. evaluation by in vivo stress relaxation. *Plant Physiol.*, 78: 347–356, 1985.
12. Ch Darwin. *The Movements and Habits of Climbing Plants*. Appleton, New York, 1888.
13. A. Delfino, N. Stergiopulos, J. E. Moore, and J. J Meister. Residual strain effects on the stress field in a thick wall finite element model of the human carotid bifurcation. *J. Biomech.*, 30: 777–786, 1997.
14. A. DiCarlo and S. Quiligotti. Growth and balance. *Mech. Res. Comm.*, 29: 449–456, 2002.
15. M. Epstein and G. Maugin. Thermomechanics of volumetric growth in uniform bodies. *Int. J. Plasticity*, 16: 951–978, 2000.
16. H. Frieboes, X. Zheng, C. H Sun, B. Tromberg, R. Gatenby, and V. Cristini. An integrated computational/experimental model of tumor invasion. *Cancer Research*, 66: in press, 2006.
17. Y. B. Fu and R. W. Ogden. *Nonlinear Elasticity. Theory and applications*. Cambridge University Press, Cambridge, 2001.
18. Y. C Fung. Stress, strain, growth, and remodeling of living organisms. *Z. angew. Math. Phys.*, 46 (special issue): S469–S482, 1995.
19. A. Gent. A new constitutive relation for rubber. *Rubber Chem. and Technol.*, 69: 59–61, 1996.
20. A. N. Gent. Elastic instabilities in rubber. *Int. J. Non-Linear Mech.*, 40: 165–175, 1995.
21. R. Goldstein and A. Goriely. The morphoelasticity of tendrils. *Phys. Rev. E*, 74: #010901, 2006.
22. B. C. Goodwin and C. Briere. A mathematical model of cytoskeletal dynamics and morphogenesis in acetabularia. In D. Menzel, editor, *The Cytoskeleton of the Algae*, 219–233. CRC Press, Boca Raton, 1992.
23. A. Goriely and M. Ben Amar. On the definition and modeling of incremental, cumulative, and continuous growth laws in morphoelasticity. *Biomechanics and Modeling in Mechanobiology*, To be published, 2006.
24. A. Goriely and M. Ben Amar. Differential growth and instability in elastic shells. *Phys. Rev. Lett.*, 94: #198103, 2005.

25. A. Goriely and S. Neukirch. The mechanics of climbing and attachment in twining plants. *Phys. Rev. Lett.*, To be published: 1–4, 2006.
26. A. Goriely and M. Tabor. Nonliner dynamics of filaments. *Nonlinear Dynamics*, 21: 101–133, 2000.
27. A. Goriely and M. Tabor. New amplitude equations for thin elastic rods. *Phys. Rev. Lett.*, 77: 3537–3540, 1996.
28. A. Goriely and M. Tabor. Nonlinear dynamics of filaments IV: The spontaneous looping of twisted elastic rods. *Proc. Roy. Soc. London (A)*, 455: 3183–3202, 1998.
29. A. Goriely, M. Nizette, and M. Tabor. On the dynamics of elastic strips. *J. Nonlinear Science*, 11: 3–45, 2001.
30. D. M. Haughton and R. W. Ogden. On the incremental equations in non-linear elasticity-II. Bifurcation of pressurized spherical shells. *J. Mech. Phys. Solids*, 26: 111–138, 1978.
31. D. M. Haughton and R. W. Ogden. Bifurcation of inflated circular cylinders of elastic material under axial loading-I. Membrane theory for thin-walled tubes. *J. Mech. Phys. Solids*, 27: 489–512, 1979.
32. D. M. Haughton and A. Orr. On the eversion of compressible elastic cylinders. *Int. J. Solids Structures*, 34: 1893–1914, 1997.
33. G. Helmlinger, P. A. Netti, H. C. Lichtenbeld, R. J. Melder, and R. K. Jain. Solid stress inhibits the growth of multicellular tumor spheroids. *Nature Biotech.*, 15: 778–783, 1997.
34. G. A. Holzapfel, T. C. Gasser, and R. W. Ogden. A new constitutive framework for arterial wall mechanics and a compartaive study of material models. *J. Elasticity*, 61: 1–48, 2000.
35. C. 0. Horgan and G. Saccomandi. A molecular-statistical basis for the Gent constitutive model of rubber elasticity. *J. Elasticity*, 68: 167–176, 2002.
36. C. 0. Horgan and G. Saccomandi. Constitutive modeling of rubber-like and biological materials with limited chain extensibility. *Math. Mech. Solids*, 7: 353–371, 2002.
37. C. 0. Horgan and G. Saccomandi. A description of arterial wall mechanics using limiting chain extensibility constitutive models. *Biomechan. Model Mechanobiol.*, 1: 251–266, 2003.
38. C. 0. Horgan and G. Saccomandi. Constitutive models for compressible nonlinearly elastic materials with limiting chain extensibility. *J. Elasticity*, 77: 123–138, 2004.
39. F. H Hsu. The influences of mechanical loads on the form of a growing elastic body. *J. Biomech.*, 1: 303–311, 1968.
40. J. D. Humphrey and K. R. Rajagopal. A constrained mixture model for growth and remodeling of soft tissues. *Math. Models. Meth. Appl. Sci.*, 12: 407–430, 2002.
41. I. Klapper. Biological applications of the dynamics of twisted elastic rods. *J. Comp. Phys.*, 125: 325–337, 1996.
42. I. Klapper and M. Tabor. Dynamics of twist and writhe and the modeling of bacterial fibers. In J. Mesirov, K. Schuiten, and De Witt Summers, editors, *Mathematical Approaches to Biomolecular Structure and Dynamics*, 139–159. Springer, 1996.
43. S. M. Klisch, T. J. Van Dyke, and A. Hoger. A theory of volumetric growth for compressible elastic biological materials. *Math. Mech. Solids*, 6: 551–575, 2001.

44. E. H. Lee. Elastic-plastic deformation at finite strains. *J. Appl. Mech.*, 36: 1–8, 1969.
45. J. A. Lockhart. An analysis of irreversible plant cell elongation. *J. Theor. Biol.*, 8: 264–275, 1965.
46. B. D. MacArthur and C. C. Please. Residual stress generation and necrosis formation in multicell tumour spheroids. *J. Math. Biol.*, 49: 537–552, 2004.
47. J. H. Maddocks. Bifurcation theory, symmetry breaking and homogenization in contiunuum mechanics descriptions of DNA. In M. J. Givoli D. Grote and G. Papanicolaou, editors, *A Celebration of Mathematical Modeling: The Joseph B. Keller Anniversary Volume*, pages 113–136. Kluwer,, 2004.
48. A. A. Matista and W. K. Silk. An electronic device for continuous, in vivo measurement of forces exerted by twining vines. *Am. J. Bot.*, 84: 1164–1168, 1997.
49. G. A. Maugin. Pseudo-plasticity and pseudo-inhomogeneity effects in material mechanics. *J. Elasticity*, 71: 81–103, 2003.
50. T. McMillen and A. Goriely. Tendril perversion in intrinsically curved rods. *J. Nonlinear Science*, 12: 241–281, 2002.
51. N. H. Mendelson. Helical *Bacillus subtilis* macrofibers: morphogenesis of a bacterial multicellular macroorganism. *Proc. Natl. Acad. Sci. USA*, 75: 2472–2482, 1978.
52. N. H. Mendelson. Bacterial macrofibers: the morphogenesisof complex multicellular bacterial forms. *Sci. Progress Oxford*, 74: 425–441, 1990.
53. N. H. Mendelson. *Bacillus subtilis* macrofibres, colonies and bioconvection patterns use different strategies to achieve multicellular organization. *Environmental microbiol.*, 1: 471–478, 1999.
54. F. Michor, Y. Iwasa, and M. A. Nowak. Dynamics of cancer progression. *Nature Rev. Cancer*, 4: 197–205, 2004.
55. P. M. Naghdi. A critical review of the state of finite plasticity. *Zeitschrift fr Angewandte Mathematik und Physik*, 41: 315–394, 1990.
56. R. W. Ogden. *Non-linear elastic deformation*. Dover, New york, 1984.
57. R. W. Ogden and A. Guillou. *Growth in soft biological tissue and residual stress developments*. Preprint, 2005.
58. J. K. E. Ortega. Augmented growth equation for cell wall expansion. *Plant Physiol.*, 79: 318–320, 1985.
59. A. Rachev. Theoretical study of the effect of stress-dependent remodeling on arterial geometry under hypertensive conditions. *J. Biomech.*, 30: 819827., 1997.
60. E. K. Rodriguez, A. Hoger, and McCulloch A. Stress-dependent finite growth in soft elastic tissue. *J. Biomechanics*, 27: 455–467, 1994.
61. T. Roose, P. A. Netti, L. L. Munn, Y. Boucher, and R. K. Jain. Solid stress generated by spheroid growth estimated using a linear poroelasticity model. *Microvascular R.*, 66: 204–212, 2003.
62. M. S. Sacks. Biaxial mechanical evaluation of planar biological materials. *J. Elasticity*, 61: 199–246, 2000.
63. M. Sarntinoranont, F. Rooney, and M. Ferrari. Interstitial stress and fluid pressure within a growing tumor. *Annals biomed. Eng.*, 31: 327–335, 2003.
64. J. L. Scher, MN M. Holbrook, and W. K. Silk. Temporal and spatial patterns of twining force and lignification in *Ipomoea purpurea*. *Planta*, 213: 192–198, 2001.
65. A. P. S. Selvadurai. Deflections of a rubber membrane. *J. Mech. Phys. Solids*, 54: 1093–1119, 2006.

66. O. A. Shergold, N. A. Fleck, and D. Radford. The uniaxial stress versus strain response of pig skin and silicone rubber at low and high strain rates. *Int. J. of Impact Eng.*, 32: 1384–1402, 2006.
67. B. I. Shraiman. Mechanical feedback as a possible regulator of tissue growth. *Proc. Natl. Acad. Sci. USA*, 102: 3318–3323, 2005.
68. W. K. Silk. Growth rate patterns which maintains a helical tissue tube. *J. Theor. Biol.*, 138: 311–327, 1989.
69. W. K. Silk and N. M. Holbrook. The importance of frictional interaction in maintaining the stability of the twining habit. *Amer. J. Bot.*, 92: 1820–1826, 2005.
70. W. K. Silk and M. Hubbard. Axial forces and normal distributed loads in twining stems of morning glory. *J. Biomechanics*, 24: 599–606, 1991.
71. A. A. Stein. The deformation of a rod of growing biological material under longitudinal compression. *J. Appl. Math. Mech.*, 59: 139–146, 1995.
72. L. A. Taber. Biomechanics of growth, remodeling and morphogenesis. *Appl. Mech. Rev.*, 48: 487–545, 1995.
73. L. A. Taber. Biomechanical growth laws for muscle tissues. *J. Theor. Biol.*, 193: 201–213, 1998.
74. L. A. Taber and D. W. Eggers. Theoretical study of stress-modulated growth in the aorta. *J. Theor. Biol.*, 180: 343–357, 1996.
75. D. Wodarz and N. L. Komarova. *Computational biology of cancer: Lecture notes and mathematical modeling*. World Scientific, Singapore, 2005.
76. C. W. Wolgemuth, R. E. Goldstein, and T. R. Powers. Dynamic supercoiling bifurcation of growing elastic filaments. *Phys. D*, 190: 266–289, 2004.
77. H. Xiao, T. O. Bruhns, and A. Meyers. Elastoplasticity beyond small deformations. *Acta Mechanica*, 182: 31–111, 2006.